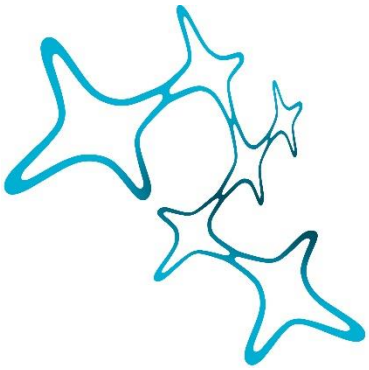

Graduate School of
Systemic Neurosciences
LMU Munich

Imaging Markers of Cerebral Small Vessel Disease

Ebru Baykara

Dissertation

der Graduate School of Systemic Neurosciences

der Ludwig-Maximilians-Universität München

Munich, April 2018

First Reviewer:	PD Dr. med. Marco Düring
Second Reviewer:	Prof. Dr. Stefan Glasauer
Date of Submission:	20.04.2018
Date of Defense:	06.08.2018

Table of Contents

SUMMARY

Vascular cognitive impairment (VCI) is the second most common cause of cognitive impairment in the elderly population and it very often co-occurs with impairment resulting from other neurodegenerative pathologies. Cognitive impairment due to vascular pathology is potentially treatable; i.e. the progression could be slowed or even stopped by managing the underlying vascular disease. However, there is no specific treatment available for VCI up to date. One of the main reasons for this is an insufficient understanding of the disease pathophysiology.

Cerebral small vessel disease is the primary pathology leading to VCI and therefore its study provides the chance to elucidate the mechanisms leading from vascular pathology to cognitive impairment. Understanding the underlying disease mechanisms is crucial for diagnosis, prevention and managing the disease. For this purpose, markers play an important role, as they indicate which disease processes are at play within the brain.

This PhD-work aimed at finding optimal imaging markers for diagnosing cerebral small vessel diseases and estimating the vascular disease burden in the brain. Advances in brain imaging tools, in particular diffusion tensor imaging (DTI), have enabled the exploration of microstructural changes in the human brain, which precede the occurrence of lesions that are visible on conventional MRI. The first project focused on developing and establishing a DTI-based imaging marker for small vessel disease that is quantitative, reliable, and fully automated. This marker (peak width of skeletonized mean diffusivity, PSMD) was then systematically investigated - along with conventional imaging markers - in patients with hereditary and sporadic SVD, memory clinic patients as well as in patients with Alzheimer pathology. The results showed that PSMD outperformed the conventional markers in explaining the cognitive impairment scores. Furthermore, in longitudinal analysis, PSMD was more sensitive to disease related changes than any other imaging markers, which resulted in low sample size estimations for a hypothetical clinical trial. Additionally. PSMD showed very high interscanner reproducibility suggesting that it might be especially useful in multicenter studies. Interestingly, increases in PSMD were mostly linked to vascular but not to neurodegenerative disease. Therefore, PSMD could be a valuable tool to disentangle effects caused by these different pathologies, a common challenge in understanding cognitive

impairment. This suggests that the newly established marker PSMD could be easily applied to large samples and may be of great utility for both research studies and clinical use.

The second project focused on the evaluation of cortical superficial siderosis (cSS) as a potential new marker for cerebral small vessel diseases. cSS emerged recently as a marker for cerebral amyloid angiopathy (CAA). However, the presence of cSS is associated with many other signs of cSVD, such as cerebral microbleeds (CMB) and white matter hyperintensities (WMH), and therefore its specificity for CAA was questionable. The results of the second project revealed that the distribution patterns and frequency of CMB and WMH overlap between different subtypes of cSVD. This clearly demonstrated that these imaging features have limited discriminative value. More importantly, the presence of cSS was found to be strongly indicative of CAA.

To summarize, the key findings reported in this PhD-work have important implications for diagnosing patients with cerebral small vessel disease, disentangling underlying pathologies, as well as for managing and treating the disease. The newly established imaging marker PSMD can be utilized to select the target population for clinical studies and may function as a surrogate marker for treatment effects. PSMD can be further used to identify patients who have a low disease burden as targets for prevention and early treatment.

INTRODUCTION

Vascular cognitive impairment (VCI), or cognitive decline due to vascular pathology, is the second most common cause of dementia after Alzheimer's disease and it is a major health concern for the aging populations. In most of the VCI cases, small vessel disease is the underlying cerebral pathology (Pantoni, 2010). Cerebral small vessel disease (cSVD) is an umbrella term used for the various disease subtypes where the small vessels in the brain are affected. The term embraces the whole spectrum of related clinical and imaging abnormalities (Pantoni, 2010). The disease itself can be undetected for many years, and so far, there is no available treatment specific for cSVD. There are currently several studies investigating the effects of lifestyle changes and manipulation of vascular risk factors on cSVD; however, the results remain inconclusive (the largest treatment study up to date: the Secondary Prevention of Small Subcortical Strokes (SPS3) study, Benavente et al., 2011; for reviews see Bath & Wardlaw, 2015; Dichgans & Zietemann, 2012).This is in part due to inadequate understanding of the disease pathophysiology. It is therefore of great importance to understand the disease mechanisms to facilitate early diagnosis, optimisation of prevention strategies and provide management of the disease. Furthermore, the pathology of cSVD very often co-occurs with Alzheimer's disease (AD), and both diseases share common risk factors. It is difficult to differentiate the contribution of vascular pathology from Alzheimer pathology; however, for managing and treating cSVD this differentiation is crucial (Wardlaw et al., 2013b).

The purpose of the studies presented in this thesis was to identify optimal imaging markers for reliable diagnosis of cerebral small vessel disease as well as for the estimation of the vascular burden in the brains of affected patients. The first project also aimed at establishing an imaging marker that would separate the contribution of vascular pathology from AD pathology.

In the following chapters, there will be an overview of the two main types of cerebral small vessel disease (cSVD), the associated clinical characteristics and their underlying pathologies. Furthermore, the existing imaging markers utilised in the field of cSVD will be introduced and discussed regarding their strengths and weaknesses, in order to justify the need for a new imaging marker and lay the groundwork for the research questions in the present thesis.

1.1. Pathogenesis of cerebral small vessel disease

It is very important to know the underlying disease physiology to have a clear understanding of the disease, the main risk factors, and possible treatment strategies. The pathophysiology of cSVD involves thickening and stiffness of and damage to the vessel walls, luminal narrowing, hypoperfusion, disturbed vasoreactivity and autoregulation, which can all result in the occlusion, leakage or rupture of small vessels in the brain (Wardlaw, Smith, & Dichgans, 2013a). Chronic hypoperfusion and ischaemia consequent to the aforementioned pathologies are thought to lead to diffuse alterations in the white matter. Alternatively, they can lead to lacunar infarcts in the case of complete occlusion of the lumen resulting in focal acute and severe ischaemia (Pantoni, 2002). Furthermore, vessel leakage or rupture resulting from vessel wall damage, microaneurysms, or amyloid deposition can result in micro- or macrohemorrhages (Pantoni, 2010). Brain atrophy is also one of the signs of cSVD and it can also occur as a remote consequence of vascular pathology (Duering et al., 2012; Jouvent et al., 2007). A widely accepted model of the pathogenesis of cSVD is presented in Figure 1; however, it is important to consider that this model is now challenged by recent studies. One study investigated the spatial relationships between lacunes and white matter hyperintensities and showed that lacunes appear in the proximity of existing white matter hyperintensities, thus suggesting that their mechanisms are intimately linked (Duering et al., 2013a).

1.1.1 Types of cerebral small vessel disease

The most frequently seen types of cSVD are (1) arteriolosclerosis (age- and vascular risk factor-related small vessel diseases) and (2) cerebral amyloid angiopathy (Pantoni, 2010), and these subtypes are the focus of this thesis in investigating new imaging markers.

1.1.1.1. Arteriolosclerosis

The most common type of cSVD is arteriolosclerosis, which is related to ageing and vascular risk factors, in particular diabetes and hypertension. The pathological findings related to arteriolosclerosis are degeneration of smooth muscle cells in the tunica media and deposition of fibrohyaline substance that results in a loss of elasticity of the vessels, thickening of the vessel walls and also potentially in narrowing of the lumen (Pantoni, 2010).

CADASIL

Hereditary forms of arteriolosclerosis are also increasingly recognised. Cerebral Autosomal

Dominant Arteriopathy with Subcortical Infarcts and Leukoencephalopathy (CADASIL) is the most common hereditary cause of stroke and cognitive decline, and has thus gained great interest as the model disease to study the more common sporadic form of cSVD (Chabriat, Joutel, Dichgans, Tournier-Lasserve, & Bousser, 2009). CADASIL shares the clinical and neuroimaging features of sporadic cSVD, with an earlier onset and a more severe prognosis (Chabriat et al., 2009; Charlton, Morris, Nitkunan, & Markus, 2006).

CADASIL is an autosomal dominant disease caused by mutations in *NOTCH3*, which encodes for a transmembrane receptor protein (Joutel et al., 1996). *NOTCH3* is predominantly expressed in vascular smooth muscle cells and it has a critical role for the structural and functional integrity of small vessels (Joutel et al., 1996, 2000). The arteriopathy related to CADASIL is characterised mainly by the thickening of the arterial walls, the deposition of a non-amyloid granular osmiophilic material in the arterial walls, and prominent degeneration of vascular smooth-muscle cells (Chabriat et al., 2009). CADASIL causes stroke and dementia, and leads to a particular pattern of diffuse white matter hyperintensities on brain imaging, typically also in the anterior part of the temporal lobes (O'Sullivan et al., 2001). CADASIL can be diagnosed either by skin biopsy or by molecular genetic testing (Joutel et al., 1996; Peters et al., 2005). For the present thesis, we used CADASIL as a model disease to study arteriolosclerosis, as it represents a pure form of the disease without other age-related diseases as concomitant pathologies.

1.1.1.2. Cerebral amyloid angiopathy (CAA)

Cerebral amyloid angiopathy (CAA) is a common age-related small vessel disease and a major risk factor for intracerebral haemorrhage (ICH) and cognitive impairment (Viswanathan & Greenberg, 2011).

Additionally, CAA very often coexists with Alzheimer's disease (Kalaria & Ballard, 1999). The pathological hallmark of the disease is the accumulation of amyloid beta protein in the walls of arteries and arterioles found in leptomeningeal and cortical areas. This leads to vessel fragility, rupture and bleeding (Vinters, 1983). Alternatively, amyloid beta deposits can alter the stiffness of vessel wall, which leads to decreased cerebrovascular reactivity and results in hypoperfusion. Although most of the research is focused on the more frequent and recurrent haemorrhagic manifestations of the disease, ischemic changes are also observed in CAA patients and are clinically relevant (Reijmer, van Veluw, & Greenberg, 2016).

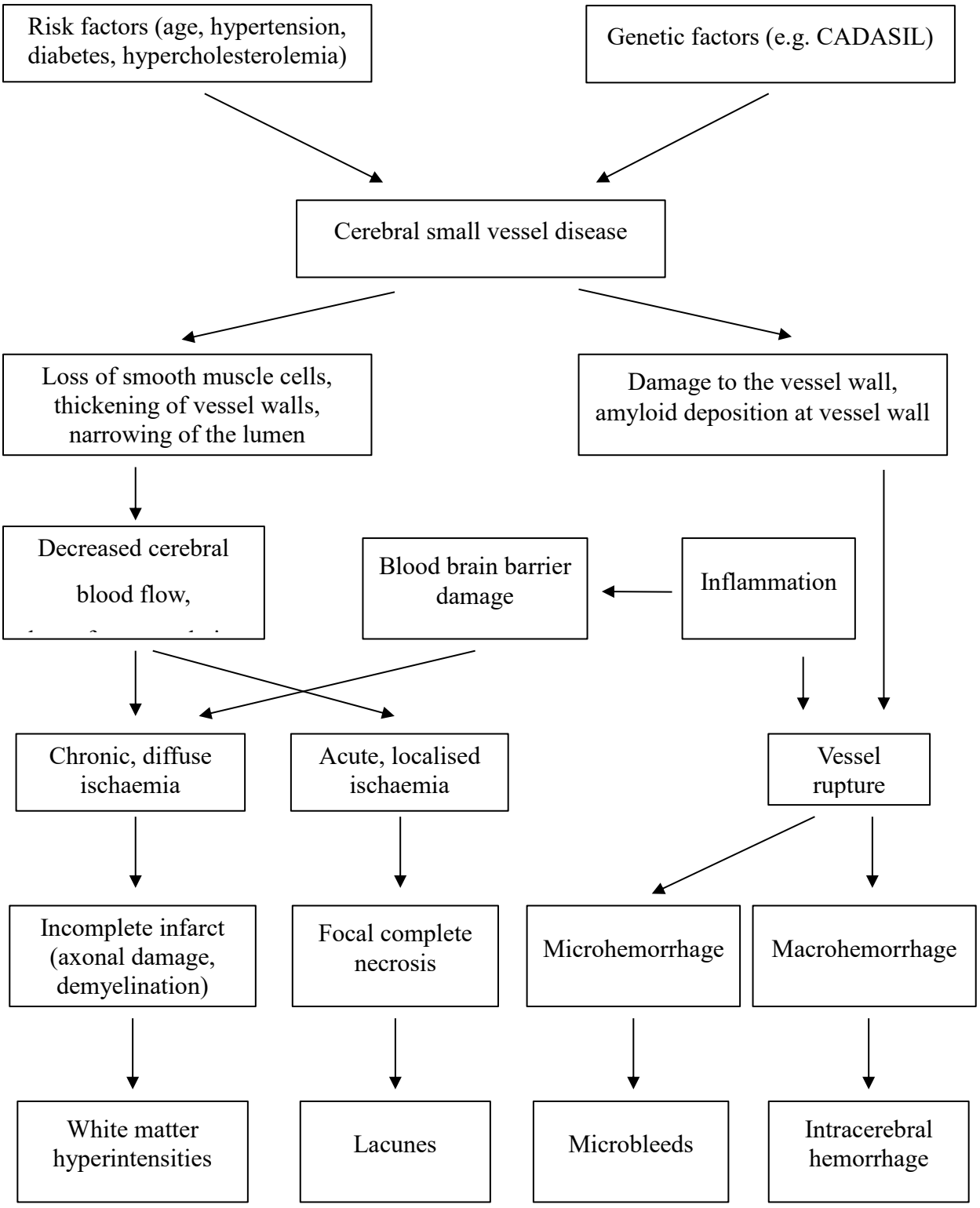

Figure 1. Pathogenesis of cerebral small vessel disease (adapted from Pantoni, 2010)

Table 1. Classic and modified Boston criteria for CAA (Linn et al., 2010)

	Classic Boston Criteria	Modified Boston Criteria
Definite CAA	Full postmortem examination demonstrating:	No modification compared to the classic Boston criteria
	Lobar, cortical or corticosubcortical hemorrhage	
	Severe CAA with vasculopathy	
	Absence of other diagnostic lesions	
Probable CAA with supporting pathology	Clinical data and pathologic tissue (evacuated hematoma or cortical biopsy) demonstrating:	No modification compared to the classic Boston criteria
	Lobar, cortical, or corticosubcortical hemorrhage	
	Some degree of CAA in specimen	
	Absence of other diagnostic lesion	
Probable CAA	Clinical data and MRI or CT demonstrating:	Clinical data and MRI or CT demonstrating:
	Multiple hemorrhages restricted to lobar, cortical, or corticosubcortical regions (cerebellar hemorrhage allowed)	Multiple hemorrhages restricted to lobar, cortical, or corticosubcortical regions (cerebellar hemorrhage allowed) or
		Single lobar, cortical, or corticosubcortical hemorrhage and focal[a] or disseminated[b] superficial siderosis
	Age ≥ 55 y	Age ≥ 55 y
	Absence of other cause of hemorrhage	Absence of other cause of hemorrhage or superficial siderosis
Possible CAA	Clinical data and MRI or CT demonstrating:	Clinical data and MRI or CT demonstrating:
	Single lobar, cortical, or corticosubcortical hemorrhage	Single lobar, cortical, or corticosubcortical hemorrhage
		Focal[a] or disseminated[b] superficial siderosis
	Age ≥ 55 y	Age ≥ 55 y
	Absence of other cause of hemorrhage	Absence of other cause of hemorrhage or superficial siderosis

CAA = cerebral amyloid angiopathy; CT = computed tomography; MRI = magnetic resonance imaging.
[a]Siderosis restricted to 3 or fewer sulci;.[b]Siderosis affecting at least 4 sulci

For the definite diagnosis of CAA, the vascular amyloid must to be detected by histopathology, i.e. either in biopsy or autopsy. However, Boston criteria were postulated (Knudsen, Rosand, Karluk, & Greenberg, 2001) and later modified (Linn et al., 2010), enabling the clinical diagnosis during life with high specificity (see Table 1). The modified criteria include cortical superficial siderosis (cSS), which results from hemosiderin deposition in the subpial layers of the brain and which is a focus of this thesis as an emerging imaging marker for CAA.

Hereditary forms of CAA are extremely rare in the general population, and they are more severe and earlier in onset. Hereditary CAA generally cause cognitive impairment but are not necessarily presented with lobar ICH (Biffi & Greenberg, 2011). Example images of the lesions can be found in Figure 2.

1.2. Clinical characteristics of cerebral small vessel disease

1.2.1. Cognitive impairments related to cerebral small vessel disease

Cognitive impairment due to cSVD has a relatively homogenous profile and is progressive in nature. Additionally, the neuroimaging correlates of cSVD are widely investigated, and therefore cognitive impairment resulting from cSVD can be studied *in vivo* and can be a target for clinical and therapeutic trials (Pantoni, 2010).

Cognitive profile of patients with cSVD involves prominent impairments in processing speed and executive functions, with a relative sparing of memory functions (Charlton et al., 2006; Dichgans, 2009; O'Brien et al., 2003). However, since cSVD and AD can often overlap in the elderly population, a clinical differentiation of cSVD or AD from mixed disease based on neuropsychological assessment alone is challenging and misleading (Gorelick et al., 2011). Patients with the hereditary disease CADASIL share a comparable cognitive profile with patients with sporadic cSVD, and they display cognitive deficits at an early age when AD comorbidity is highly unlikely (Charlton et al., 2006). Therefore, CADASIL is a useful disease model for investigating cognitive impairment due to pure cSVD.

MRI and autopsy studies have shown that the total lesion burden and lesion location influence the clinical expression of cSVD, particularly the cognitive profile of the patients (Gold, 2009). The lesion volumes explain only a moderate amount of the variation in the

cognitive scores, and studies demonstrated that lesions on strategic white matter pathways (Duering et al., 2011, 2014) (anterior thalamic radiation and forceps minor), and more generally on frontal-subcortical neuronal circuits (Duering et al., 2013b) play a crucial role on the development of cSVD related cognitive deficits.

1.2.2. Other impairments related to cerebral small vessel disease

Other than cognitive impairments, cSVD patients experience gait, mood, behavioural and urinary disturbances (Pantoni, 2010). Like the cognitive decline, these disturbances are progressive and patients can lose their autonomy completely in the advanced stages of the disease. They can be depressed, apathetic, unable to walk and have urinary incontinence (Pantoni, 2010). More detailed explanation of the non-cognitive impairments related to cSVD are beyond the scope of this thesis, however, it is important to acknowledge the importance of these impairments in the spectrum of the disease and their effects on the daily lives of the patients.

1.3. Prevention and Treatment

1.3.1. Prevention

The characteristic cSVD lesions are associated with stroke, mortality and functional impairment (cognitive, motor, mood, behavioural) and they are very often correlated with vascular risk factors (Pantoni, 2010). Hence, it is plausible that some of the effects of the disease are preventable and patients with VCI are an important target population for prevention. Preventive strategies include lifestyle changes (physical exercise, healthy diet, smoking cessation) and controlling vascular risk factors (hypertension, hypercholesterolemia and diabetes) (Dichgans & Leys, 2017). A longitudinal study with CADASIL patients showed that active smoking increases the risk of stroke and dementia significantly (Chabriat et al., 2016), a relation already reported previously for sporadic cSVD (Bezerra et al., 2012) and in the general population (Gons et al., 2011). Typically for people with high risk for VCI, it is recommended to quit smoking, to get treated especially for hypertension but also for hypercholesterolemia and diabetes, to control alcohol intake and weight, and also to do physical exercise (Gorelick et al., 2011). Preventing vascular disease with multi-domain interventions is so far the most promising strategy to prevent VCI and dementia, although the

evidence for the effectiveness is inconclusive (Dichgans & Zietemann, 2012). Recent studies with risk populations reported that multidomain intervention had positive effects (maintenance or even improvement) on cognitive functioning (FINGER study, Ngandu et al., 2015), whereas it did not result in diminishing progression of cerebrovascular lesions, particularly white matter hyperintensities (van Dalen et al., 2017).

1.3.2. Treatment

Currently, there are no specific treatments available for cSVD and related cognitive impairment, and there are only a few validated options. The management strategy for patients with cSVD consists generally of treating comorbidities, psychological and behavioral symptoms, and providing information to patients and their caregivers (Dichgans & Leys, 2017). The best studied symptomatic treatments for VCI are cholinesterase inhibitors and the NMDA receptor antagonist memantine, both established drugs used for Alzheimer's disease (O'Brien & Thomas, 2015). The rationale for using cholinesterase inhibitors in VCI was based on evidence for a cholinergic deficit found in the disease (Mesulam, Siddique, & Cohen, 2003). Pharmacological therapies targeting VCI have displayed consistent but modest benefits of donepezil (Black et al., 2003; Dichgans et al., 2008; Wilkinson et al., 2003), galantamine (Auchus et al., 2007) and memantine (Orgogozo, Rigaud, Stöffler, Möbius, & Forette, 2002) on cognition. However, the reported effects of these drugs on global functioning and daily living have been less consistent. Therefore, considering the small beneficial effect of these drugs on VCI symptoms and their possible side effects, regulatory bodies do not recommend cholinesterase inhibitors and memantine for patients with VCI or vascular dementia (VaD) (NICE, 2007; O'Brien & Thomas, 2015).

1.4. Magnetic resonance imaging of cerebral small vessel disease

The small vessels affected in the disease cannot be visualized *in vivo* with brain imaging in the living brain, therefore parenchymal abnormalities associated with cSVD and detected on magnetic resonance imaging (MRI) are used as markers of the presence, severity and progression of the disease (Pantoni, 2010). In this section, the existing imaging markers will be introduced. Although all these markers offer important information about the disease and its underlying pathophysiology, there is a pressing need for a new imaging marker that can

overcome the weaknesses of these markers, which are described in the following section.

1.4.1. Ischaemic manifestations of the disease

1.4.1.1. White matter hyperintensities of presumed vascular origin

White matter hyperintensities (WMH) can be detected as increased signal on T2- weighted and fluid attenuated inversion recovery (FLAIR) MR images and often as decreased signal on T1-weighted images (Wardlaw et al., 2013b). Studies have revealed that WMH are associated with physical (de Laat et al., 2011; Sachdev, 2005) and cognitive impairments (Prins & Scheltens, 2015), and also with the risk of stroke and dementia (Debette & Markus, 2010).

There are heterogeneous pathophysiological changes associated with WMH. Pathological findings related to WMH are tissue rarefaction of myelin sheaths, loss of axons and alternatively, changes in the cerebrospinal fluid (CSF) circulation or disturbances of the blood-brain barrier (Pantoni & Garcia, 1997). Despite the heterogeneity in the pathogenesis of white matter lesions, most studies relate these lesions to ischaemic brain damage resulting from cSVD and cerebrovascular risk factors such as arterial hypertension and diabetes mellitus (Debette & Markus, 2010).

The severity of WMH can be assessed by visual rating scales (e.g. Fazekas scale, Fazekas, Chawluk, Alavi, Hurtig, & Zimmerman, 1987, or Wahlund scale, Wahlund et al., 2001) taking into account the location and extent of the lesions. However, quantitative WMH assessment (WMH volumetry) is more reproducible and sensitive for lesion progression than the visual scales (Gouw et al., 2008). Nevertheless, visual ratings and also volumetric assessments of WMH are only moderately associated with the clinical status, particularly cognitive impairment (de Groot et al., 2000; Duering et al., 2011).

A very likely explanation for the weak association with clinical symptoms is that the tissue damage with varying degrees can appear as WMH in the MR imaging (Fazekas et al., 1993). Therefore, these lesions should be carefully interpreted. It is also repeatedly shown that tissue, which appears normal in MRI, is not necessarily healthy but could already have undergone pathological changes. Thus, WMH detected on structural MRI is not a true reflection of tissue damage in the brain, and the true white matter pathology is likely to be more extensive (de Groot et al., 2013). That is also one reason why there is a need for more optimal disease markers. Furthermore, the semi-automated methods of WMH quantification

require manual editing that is highly subjective and time consuming, and thus preclude the usage of WMH as a marker for large-scale studies.

1.4.1.2. Lacunes of presumed vascular origin

Lacunes of presumed vascular origin are round, subcortical, fluid-filled (similar intensity signal as CSF) cavities, between 3 to 15 mm in diameter. Lacunes result mostly from symptomatic or silent small subcortical infarcts, and to a lesser degree from small deep hemorrhages (Wardlaw et al., 2013b). Studies showed that lacunes are associated with increased risk of stroke and dementia (Vermeer, Longstreth, & Koudstaal, 2007).

Semi-automated quantitative measures for lacune detection are available; however, manual corrections are needed. Perivascular spaces (also known as Virchow–Robin spaces) may appear very similar to lacunes on MR imaging, and differentiation of these two lesion types can be very difficult even for experts (Wardlaw et al., 2013b). Greatly enlarged perivascular spaces (EPVS) can be even larger than 2cm and are mostly located below the putamen (Wardlaw et al., 2013b). It has also been shown that EPVS are another MRI marker of cSVD and therefore are likely to co-occur with lacunes and other markers of the disease (Doubal, MacLullich, Ferguson, Dennis, & Wardlaw, 2010).

Typical measurements of interest for lacunes are the number, size and location of the lesions. Since the spread of MR imaging, the prevalence of lacunes in the general population has been found to be higher than initially thought. A majority of these small brain infarcts remain asymptomatic since they are not located on strategic brain regions (Duering et al., 2013b). Although these lesions lack overt symptoms, they are still associated with subtle deficits and with an increased risk of subsequent stroke, cognitive impairment and dementia (Vermeer et al., 2007).

Although the number and size of lacunes may be a marker for disease severity, their detection is time-consuming and the number of detected lacunes depends on the rater, as it is difficult to differentiate them from EPVS. Therefore, lacunes are not well suited as disease markers.

1.4.2. Hemorrhagic manifestations of the disease

1.4.2.1. Microlesions

Cerebral Microbleeds

The radiologically defined cerebral microbleeds (CMBs) are small signal voids (black or hypointense lesions) as seen on MRI sequences sensitive to susceptibility effects (T2* or susceptibility weighted MR images). As suggested by histopathology studies, the CMBs correlate with blood-breakdown products, which result likely from blood leakage into the brain parenchyma from damaged or fragile small vessels of the brain (Shoamanesh, Kwok, & Benavente, 2011).

Although CMBs were believed to be asymptomatic by themselves, extensive research has shown that they are correlated with other manifestations of cSVD and are associated with cognitive impairment (Poels et al., 2012). The presence of CMBs correlates with cSVD, dementia and normal ageing; and is far more common in the community-dwelling elderly than initially thought. CMBs have emerged as potential imaging markers of bleeding-prone small vessels in the brain. In the cSVD populations, the prevalence of CMBs are clinically relevant since they are related to the severity of the disease; and an increased risk of future ischaemic stroke and intracerebral hemorrhage (Greenberg, Eng, Ning, Smith, & Rosand, 2004; Thijs et al., 2010). Because arteriolosclerosis and CAA have differential topographic preference, CMBs associated with these different subtypes of cSVD are expected to follow the same topographic distribution: strictly lobar (cortical-subcortical regions of brain lobes and cerebellum) in CAA; strictly deep (deep white matter, basal ganglia, thalamus, brainstem, cerebellum) in arteriolosclerosis (Martinez-Ramirez et al., 2015). However, there is not enough evidence to attribute a high diagnostic value to the spatial pattern of CMB.

Despite extensive research on the association between CMB and SVD, there are some major drawbacks of using CMB as disease marker: (1) the number of detected CMBs depend strongly on the MRI parameters like spatial resolution and magnetic field strength (Nandigam et al., 2009). (2) The prevalence of CMBs is underestimated by routine clinical MRI and false positives are not uncommon (Haller et al., 2016). (3) There is currently no method available for automatic detection of CMBs (Wardlaw et al., 2013b). Additionally, there are several mimics of CMBs such as calcification, iron deposits, and vessels on cross-section that can be mistaken for CMBs by inexperienced raters and may cause

misjudgements. In contrast, CMBs can be easily differentiated from small spontaneous intracerebral hemorrhage (ICH) because ICHs are larger and visible on T1-, T2-weighted and FLAIR sequences (Wardlaw et al., 2013b).

1.4.2.2. Macrolesions

Intracerebral Hemorrhage (ICH)

Intracerebral hemorrhage (ICH) can be a manifestation of cSVD and the recommended term to use is spontaneous ICH presumably due to SVD (Wardlaw et al., 2013b). ICHs account for approximately 12% of all strokes and have a very high rate of mortality (Qureshi et al., 2001). Studies have shown that patients with hypertensive SVD and CAA constitute a significant proportion of cases with spontaneous ICH (Yates et al., 2014). It is important to know the underlying type of vascular disease, and as with the CMBs the distinction is usually made between lobar and non-lobar hemorrhages, the former being associated with CAA and the latter with arteriolosclerosis (Wardlaw et al., 2013b).

Cortical Superficial Siderosis (cSS)

The term cortical superficial siderosis refers to neuroimaging signs of blood in the superficial cortex under the pia mater (Kumar, 2007). It can be seen on T2* or susceptibility weighted imaging (MRI sequences sensitive to susceptibility effects) as hypointense lines following the contour of the cortical surface. Revised research criteria for CAA include cSS as an additional haemorrhagic manifestation of cerebral amyloid angiopathy (Linn et al., 2010). In ratings, the location of the siderosis and the number of sulci involved (focal vs. disseminated) should be described, since it is relevant for the clinical correlates of siderosis (Linn et al., 2010).

The prevalence of cSS is very low in the general population (Vernooij et al., 2009); it gets higher among people with cognitive impairments (Wollenweber et al., 2014) and even higher among patients with previous ICH (Charidimou et al., 2013). The highest prevalence rates of cSS are reported among patients with CAA: with up to 60% of cases with definite, i.e. histopathologically proven, CAA (Linn et al., 2010).In addition to the clear link between cSS and CAA, cSS is also associated with the risk of ICH (Linn et al., 2013). What remains unknown is whether cSS is also present in other types of cSVD, e.g. arteriolosclerosis (Project 2).

1.4.3. Brain Atrophy

Brain atrophy can be global or local, and the underlying pathological mechanisms, as well as the underlying diseases, are heterogeneous (Wardlaw et al., 2013b). It can be best evaluated on T1-weighted structural MR images and it usually consists of shrinkage of brain parenchyma, cortical thinning and increase in CSF volume (in ventricles or external to the brain parenchyma).

Brain atrophy is a part of normal aging; however, this process can be modulated or accelerated by different diseases, such as neurodegenerative (e.g. Alzheimer's disease: Frisoni, Fox, Jack, Scheltens, & Thompson, 2010), demyelinating (e.g. multiple sclerosis: Benedict & Zivadinov, 2011) or cerebrovascular diseases (Schmidt et al., 2005). Many imaging studies demonstrated that there is an association between brain atrophy and cSVD, both in hereditary (Peters et al., 2006) and sporadic (Nitkunan, Lanfranconi, Charlton, Barrick, & Markus, 2011) forms of the disease. Brain atrophy has been also shown to correlate with cognitive impairment; a finding, which suggests that brain atrophy could be a potential surrogate disease marker (Nitkunan, Barrick, Charlton, Clark, & Markus, 2008; Viswanathan et al., 2010). In the context of cerebrovascular disease and cognitive impairment, the processes leading to atrophy are likely remote consequences of vascular lesions. A very plausible mechanism is secondary cortical neurodegeneration as a direct result of subcortical ischemic lesions, and evidence for this theory arose from studies revealing cortical thinning in the connected regions to an incident lacune or subcortical infarct (Duering et al., 2012), in addition to degeneration of connecting white matter tracts (Duering et al., 2015). Thus, it seems possible that brain atrophy has some mediating effect on the relation between cSVD and cognitive decline (Duering et al., 2012).

Although brain atrophy reflects a clinically important aspect of cSVD, it is known that volume loss is a non-specific result of neuronal damage, and atrophy patterns can highly overlap between diseases. Therefore, brain atrophy (or whole brain volume in cross-sectional studies) is not a specific marker for cSVD and may not be utile in evaluating vascular disease burden.

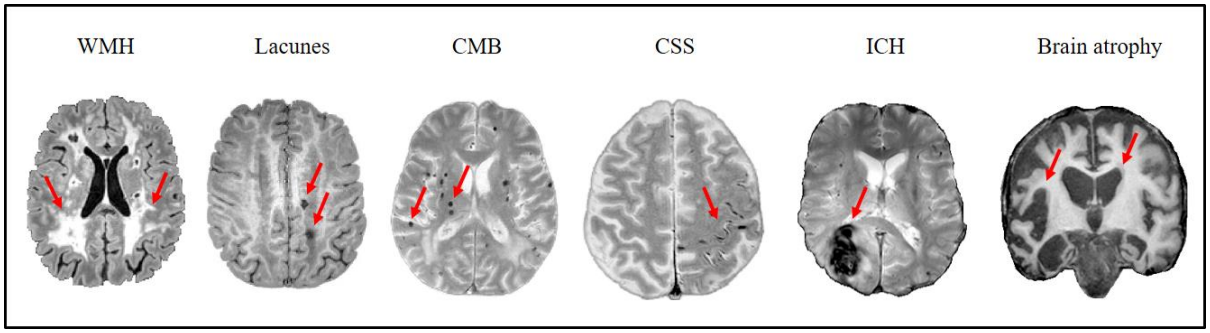

Figure 2. MRI manifestations associated with cerebral small vessel disease
Shows examples of MRI changes related to cerebral small vessel disease. Red arrows point at the lesions. CMB=cerebral microbleeds; CSS=cortical superficial siderosis; ICH=intracerebral hemorrhage; WMH=white matter hyperintensities.

1.4.4. Microstructural damage as assessed by diffusion tensor imaging

Diffusion tensor imaging (DTI) measures the diffusion of water in the brain, and is therefore a non-invasive method to measure microstructural tissue integrity (Nucifora, Verma, Lee, & Melhem, 2007). Diffusion is normally restricted by tissue boundaries (cell membranes or intracellular particles), and increase in diffusivity (mean diffusivity) together with a decrease in the directionality of diffusion (fractional anisotropy) are thought to indicate the degree of damage to white matter tracts (M O'Sullivan et al., 2004).

Studies on cSVD reported diffusion changes even in the white matter appearing normal on conventional MRI, which suggest that DTI is more sensitive towards SVD-related brain tissue damage than conventional techniques (de Groot et al., 2013). There is ample evidence to support the idea that newer, quantitative methods like DTI offer more information about the disease burden in the brain than traditional MRI sequences. In both sporadic and hereditary cSVD patients, DTI measures have been shown to correlate with cognitive deficits (Nitkunan et al., 2008; van Norden, de Laat, et al., 2012) as well as with disease progression (Holtmannspotter et al., 2005; Molko et al., 2002).

Overall, diffusion MRI provides quantitative indication of microstructural damage related to cSVD and is a promising method to assess disease burden, monitor disease progression, as well as to act as a surrogate marker to evaluate the effect of treatments in clinical trials (Project 1).

1.5. Aims of the thesis

There is a substantial vascular contribution to cognitive impairment and dementia, and small vessel disease is the most common underlying pathology. Currently, no standard disease modifying therapies are available for age- and hypertension-related cSVD (arteriolosclerosis) or CAA. As it is not possible to image *in vivo* small vessels in the brain, imaging markers are the standard for diagnosing and monitoring cSVD and assessing treatment effects. The aim of this Ph.D. work was to establish and evaluate imaging disease markers for reliable disease diagnosis, and for quantifying cSVD burden in the brain.

1.5.1. A novel imaging marker for small vessel disease based on skeletonization of white matter tracts and diffusion histograms (Project 1)

Although cSVD causes a high proportion of neurological and cognitive deficits among the elderly population, an understanding of disease pathogenesis and management of the disease have been suboptimal. The main reason is the lack of a reliable, quantitative disease marker, which is able to reflect the true disease burden in the brain. This further leads to the lack of sufficient large clinical trials for evaluating prevention and treatment strategies for the disease.

Using neuroimaging as surrogate disease marker is of great interest since the rate of cognitive decline is very slow (large samples and long follow-up periods are needed) and neuropsychological tests lose their value when repeated due to learning effects (Patel & Markus, 2011). Importantly, it has been shown that change is detectable in imaging parameters but not in cognitive scores over a short follow-up period (3 years) (Benjamin et al., 2016). Furthermore, a preclinical phase marked with changes of the brain precedes the clinical symptoms and the diagnosis of cognitive impairment and dementia. These preclinical brain abnormalities are usually observable on brain imaging. The problems with existing imaging markers are that (1) they almost always require manual editing and are therefore time-consuming and are subjective; (2) the presence of lesions in the diseased brains are potential obstacles for the algorithms used to calculate imaging markers reliably; and (3) associations with clinical symptoms, such as cognitive deficits, are typically only weak to moderate (Duering et al., 2011; Nitkunan et al., 2008). More advanced methods such as DTI can detect changes in microstructural levels, which are not yet visible on conventional MRI.

Furthermore, researchers have already shown superiority towards DTI when compared to conventional imaging markers in assessing disease burden in cSVD (van Norden, et al., 2012). However, DTI measures cannot readily be applied to large studies, since they require high amounts of post-processing. Particularly, removal of cerebrospinal fluid (CSF) from DTI data is crucial, since contamination by CSF can alter the results and be highly misleading.

The aim of this study was to establish a robust and fully-automated imaging marker for cSVD based on DTI, which can be easily implemented in studies with a large number of subjects. Our ultimate goal was to establish a disease marker that can detect the cSVD burden reliably and is highly sensitive to disease related clinical changes. We are hoping the ease of applying this marker will facilitate its application in large clinical trials for assessment of treatment effects.

1.5.2. Cortical superficial siderosis in different types of cerebral small vessel disease (Study 2)

Recently, cSS emerged as a new imaging marker for CAA. cSS is often associated with intracerebral hemorrhages, transient focal neurological episodes, cognitive deficits and dementia (Lummel et al., 2015), and therefore clinically very relevant. Other causes of cSS are known, such as vasculitis, reversible cerebral vasoconstriction syndrome or traumatic subarachnoid hemorrhage, however it is most commonly found in patients with CAA (Linn et al., 2010; Lummel et al., 2015). The presence of cSS is also associated with other typical cSVD imaging signs, particularly cerebral microbleeds and white matter hyperintensities. This raises questions about the specificity of cSS as a marker of CAA, and it remains unknown whether cSS is also present in other types of cSVD. Therefore, we analyzed the prevalence of cSS in patients with CADASIL, a model for severe non-amyloidogenic cSVD, and in subjects with age-related cSVD.

Furthermore, cSS is not the only manifestation of CAA; in addition, vascular risk factor related cSVD and CAA share many imaging disease markers. The imaging manifestations of CAA are intracerebral hemorrhages (Smith & Eichler, 2006), and microbleeds (Vernooij et al., 2008) as well as white matter hyperintensities (Gurol et al., 2013) and microinfarcts (Kimberly et al., 2009). For diagnostic purposes, it is important to distinguish between the

underlying pathologies leading to the aforementioned imaging signs of cSVD. For this purpose, we also compared the distribution of WMHs and CMBs between patients with CADASIL, age-related cSVD and probable CAA with cSS.

1.6. References

Auchus, A. P., Brashear, H. R., Salloway, S., Korczyn, A. D., De Deyn, P. P., & Gassmann-Mayer, C. (2007). Galantamine treatment of vascular dementia: A randomized trial. *Neurology*, *69*(5), 448–458. https://doi.org/10.1212/01.wnl.0000266625.31615.f6

Bath, P. M., & Wardlaw, J. M. (2015). Pharmacological Treatment and Prevention of Cerebral Small Vessel Disease: A Review of Potential Interventions. *International Journal of Stroke*, *10*(4), 469–478. https://doi.org/10.1111/ijs.12466

Benavente, O. R., White, C. L., Pearce, L., Pergola, P., Roldan, A., Benavente, M., … Hart, R. G. (2011). The Secondary Prevention of Small Subcortical Strokes (SPS3) Study. *International Journal of Stroke*, *6*(2), 164–175. https://doi.org/10.1111/j.1747-4949.2010.00573.x

Benedict, R. H., & Zivadinov, R. (2011). Risk factors for and management of cognitive dysfunction in multiple sclerosis. *Nature reviews Neurology*, *7*(6), 332–342. https://doi.org/10.1038/nrneurol.2011.61; 10.1038/nrneurol.2011.61

Benjamin, P., Zeestraten, E., Lambert, C., Chis Ster, I., Williams, O. A., Lawrence, A. J., … Markus, H. S. (2016). Progression of MRI markers in cerebral small vessel disease: Sample size considerations for clinical trials. *Journal of Cerebral Blood Flow & Metabolism*, *36*(1), 228–240. https://doi.org/10.1038/jcbfm.2015.113

Bezerra, D. C., Sharrett, A. R., Matsushita, K., Gottesman, R. F., Shibata, D., Mosley, T. H., … Selvin, E. (2012). Risk factors for lacune subtypes in the Atherosclerosis Risk in Communities (ARIC) Study. *Neurology*, *78*(2), 102–108. https://doi.org/10.1212/WNL.0b013e31823efc42

Biffi, A., & Greenberg, S. M. (2011). Cerebral Amyloid Angiopathy: A Systematic Review. *Journal of Clinical Neurology*, *7*(1), 1-9. https://doi.org/10.3988/jcn.2011.7.1.1

Black, S., Román, G. C., Geldmacher, D. S., Salloway, S., Hecker, J., Burns, A., … Pratt, R. (2003). Efficacy and tolerability of donepezil in vascular dementia: Positive results of a 24-week, multicenter, international, randomized, placebo-controlled clinical trial. *Stroke*, *34*(10), 2323–2330. https://doi.org/10.1161/01.STR.0000091396.95360.E1

Chabriat, H., Hervé, D., Duering, M., Godin, O., Jouvent, E., Opherk, C., … Dichgans, M. (2016). Predictors of clinical worsening in cerebral autosomal dominant arteriopathy

with subcortical infarcts and leukoencephalopathy: Prospective cohort study. *Stroke*, *47*(1), 4–11. https://doi.org/10.1161/STROKEAHA.115.010696

Chabriat, H., Joutel, A., Dichgans, M., Tournier-Lasserve, E., & Bousser, M.-G. (2009). CADASIL. *The Lancet Neurology*, *8*(7), 643–653. https://doi.org/10.1016/S1474-4422(09)70127-9

Charidimou, A., Jäger, R. H., Fox, Z., Peeters, A., Vandermeeren, Y., Laloux, P., … Werring, D. J. (2013). Prevalence and mechanisms of cortical superficial siderosis in cerebral amyloid angiopathy. *Neurology*, *81*(7), 626–632. https://doi.org/10.1212/WNL.0b013e3182a08f2c

Charlton, R. A., Morris, R. G., Nitkunan, A., & Markus, H. S. (2006). The cognitive profiles of CADASIL and sporadic small vessel disease. *Neurology*, *66*(10), 1523–1526. https://doi.org/10.1212/01.wnl.0000216270.02610.7e

De Groot, J. C., De Leeuw, F. E., Oudkerk, M., Van Gijn, J., Hofman, A., Jolles, J., & Breteler, M. M. B. (2000). Cerebral white matter lesions and cognitive function: The Rotterdam scan study. *Annals of Neurology*, *47*(2), 145–151. https://doi.org/10.1002/1531-8249(200002)47:2<145::AID-ANA3>3.0.CO;2-P

De Groot, M., Verhaaren, B. F. J., de Boer, R., Klein, S., Hofman, A., van der Lugt, A., … Vernooij, M. W. (2013). Changes in Normal-Appearing White Matter Precede Development of White Matter Lesions. *Stroke*, *44*(4), 1037–1042. https://doi.org/10.1161/STROKEAHA.112.680223

De Laat, K. F., Tuladhar, A. M., van Norden, A. G. W., Norris, D. G., Zwiers, M. P., & de Leeuw, F.-E. (2011). Loss of white matter integrity is associated with gait disorders in cerebral small vessel disease. *Brain*, *134*(1), 73–83. https://doi.org/10.1093/brain/awq343

Debette, S., & Markus, H. S. (2010). The clinical importance of white matter hyperintensities on brain magnetic resonance imaging: systematic review and meta-analysis. *BMJ*, *341*, c3666. https://doi.org/10.1136/bmj.c3666

Dichgans, M. (2009). Cognition in CADASIL. Stroke, *40* (3 suppl 1), S45-S47. https://doi.org/10.1161/STROKEAHA.108.534412

Dichgans, M., & Leys, D. (2017). Vascular Cognitive Impairment. *Circulation Research*, *120*(3), 573–591. https://doi.org/10.1161/CIRCRESAHA.116.308426

Dichgans, M., Markus, H. S., Salloway, S., Verkkoniemi, A., Moline, M., Wang, Q., … Chabriat, H. (2008). Donepezil in patients with subcortical vascular cognitive impairment: a randomised double-blind trial in CADASIL. *The Lancet Neurology*, *7*(4), 310–318. https://doi.org/10.1016/S1474-4422(08)70046-2

Dichgans, M., & Zietemann, V. (2012). Prevention of vascular cognitive impairment. *Stroke*, *43*(11), 3137–3146. https://doi.org/10.1161/STROKEAHA.112.651778

Doubal, F. N., MacLullich, A. M. J., Ferguson, K. J., Dennis, M. S., & Wardlaw, J. M. (2010). Enlarged Perivascular Spaces on MRI Are a Feature of Cerebral Small Vessel Disease. *Stroke*, *41*(3), 450–454. https://doi.org/10.1161/STROKEAHA.109.564914

Duering, M., Csanadi, E., Gesierich, B., Jouvent, E., Hervé, D., Seiler, S., … Dichgans, M. (2013). Incident lacunes preferentially localize to the edge of white matter hyperintensities: insights into the pathophysiology of cerebral small vessel disease. *Brain*, *136*(9), 2717–2726. https://doi.org/10.1093/brain/awt184

Duering, M., Gesierich, B., Seiler, S., Pirpamer, L., Gonik, M., Hofer, E., … Dichgans, M. (2014). Strategic white matter tracts for processing speed deficits in age-related small vessel disease. *Neurology*, *82*(22), 1946–1950. https://doi.org/10.1212/WNL.0000000000000475

Duering, M., Gonik, M., Malik, R., Zieren, N., Reyes, S., Jouvent, E., … Dichgans, M. (2013). Identification of a strategic brain network underlying processing speed deficits in vascular cognitive impairment. *Neuroimage*, *66*, 177–183. https://doi.org/10.1016/j.neuroimage.2012.10.084

Duering, M., Righart, R., Csanadi, E., Jouvent, E., Hervé, D., Chabriat, H., & Dichgans, M. (2012). Incident subcortical infarcts induce focal thinning in connected cortical regions. *Neurology*, *79*(20), 2025–2028. https://doi.org/10.1212/WNL.0b013e3182749f39

Duering, M., Righart, R., Wollenweber, F. A., Zietemann, V., Gesierich, B., & Dichgans, M. (2015). Acute infarcts cause focal thinning in remote cortex via degeneration of connecting fiber tracts. *Neurology*, *84*(16), 1685–1692. https://doi.org/10.1212/WNL.0000000000001502

Duering, M., Zieren, N., Hervé, D., Jouvent, E., Reyes, S., Peters, N., … Dichgans, M. (2011). Strategic role of frontal white matter tracts in vascular cognitive impairment: a voxel-based lesion-symptom mapping study in CADASIL. *Brain*, *134*(8), 2366–2375.

https://doi.org/10.1093/brain/awr169

Fazekas, F., Chawluk, J. B., Alavi, A., Hurtig, H. I., & Zimmerman, R. A. (1987). MR signal abnormalities at 1 . 5 T in Alzheimer ' s dementia and normal aging. *American journal of roentgenology, 149(2), 351-356*. https://doi.org/10.2214/ajr.149.2.351

Fazekas, F., Kleinert, R., Offenbacher, H., Schmidt, R., Kleinert, G., Payer, F., … Lechner, H. (1993). Pathologic correlates of incidental MRI white matter signal hyperintensities. *Neurology*, *43*(9), 1683–1689. https://doi.org/10.1212/WNL.43.9.1683

Frisoni, G. B., Fox, N. C., Jack, C. R., Scheltens, P., & Thompson, P. M. (2010). The clinical use of structural MRI in Alzheimer disease. *Nature Reviews Neurology*, *6*(2), 67–77. https://doi.org/10.1038/nrneurol.2009.215

Gold, G. (2009). Defining the Neuropathological Background of Vascular and Mixed Dementia and Comparison with Magnetic Resonance Imaging Findings. In P. Giannakopoulos, P. R. Hof (Eds.), *Dementia in Clinical Practice* (Vol. 24, pp. 86–94). Basel, Karger. https://doi.org/10.1159/000197887

Gons, R. A. R., van Norden, A. G. W., de Laat, K. F., van Oudheusden, L. J. B., van Uden, I. W. M., Zwiers, M. P., … de Leeuw, F.-E. (2011). Cigarette smoking is associated with reduced microstructural integrity of cerebral white matter. *Brain*, *134*(7), 2116–2124. https://doi.org/10.1093/brain/awr145

Gorelick, P. B., Scuteri, A., Black, S. E., DeCarli, C., Greenberg, S. M., Iadecola, C., … Seshadri, S. (2011). Vascular contributions to cognitive impairment and dementia: A statement for healthcare professionals from the American Heart Association/American Stroke Association. *Stroke*, *42*(9), 2672–2713. https://doi.org/10.1161/STR.0b013e3182299496

Gouw, A. A., van der Flier, W. M., van Straaten, E. C. W., Pantoni, L., Bastos-Leite, A. J., Inzitari, D., … Barkhof, F. (2008). Reliability and sensitivity of visual scales versus volumetry for evaluating white matter hyperintensity progression. *Cerebrovascular Diseases*, *25*(3), 247–253. https://doi.org/10.1159/000113863

Greenberg, S. M., Eng, J. A., Ning, M., Smith, E. E., & Rosand, J. (2004). Hemorrhage burden predicts recurrent intracerebral hemorrhage after lobar hemorrhage. *Stroke*, *35*(6), 1415–1420. https://doi.org/10.1161/01.STR.0000126807.69758.0e

Gurol, M. E., Viswanathan, A., Gidicsin, C., Hedden, T., Martinez-Ramirez, S., Dumas, A., … Greenberg, S. M. (2013). Cerebral amyloid angiopathy burden associated with leukoaraiosis: A positron emission tomography/magnetic resonance imaging study. *Annals of Neurology*, *73*(4), 529–536. https://doi.org/10.1002/ana.23830

Haller, S., Montandon, M.-L., Lazeyras, F., Scheffler, M., Meckel, S., Herrmann, F. R., … Kövari, E. (2016). Radiologic-histopathologic correlation of cerebral microbleeds using pre-mortem and post-mortem MRI. *Plos One*, *11*(12), e0167743. https://doi.org/10.1371/journal.pone.0167743

Holtmannspotter, M., Peters, N., Opherk, C., Martin, D., Herzog, J., Brückmann, H., … Dichgans, M. (2005). Diffusion magnetic resonance histograms as a surrogate marker and predictor of disease progression in CADASIL: a two-year follow-up study. *Stroke*, *36*(12), 2559–2565. https://doi.org/10.1161/01.STR.0000189696.70989.a4

Joutel, A., Andreux, F., Gaulis, S., Domenga, V., Cecillon, M., Battail, N., … Tournier-Lasserve, E. (2000). The ectodomain of the Notch3 receptor accumulates within the cerebrovasculature of CADASIL patients. *Journal of Clinical Investigation*, *105*(5), 597–605. https://doi.org/10.1172/JCI8047

Joutel, A., Corpechot, C., Ducros, A., Vahedi, K., Chabriat, H., Mouton, P., … Tournier-Lasserve, E. (1996). Notch3 mutations in CADASIL, a hereditary adult-onset condition causing stroke and dementia. *Nature*, *383*(6602), 707–710. https://doi.org/10.1038/383707a0

Jouvent, E., Viswanathan, A., Mangin, J.-F., O'Sullivan, M., Guichard, J.-P., Gschwendtner, A., … Chabriat, H. (2007). Brain atrophy is related to lacunar lesions and tissue microstructural changes in CADASIL. *Stroke*, *38*(6), 1786–1790. https://doi.org/10.1161/STROKEAHA.106.478263

Kalaria, R. N., & Ballard, C. (1999). Overlap between pathology of Alzheimer disease and vascular dementia. *Alzheimer Disease and Associated Disorders*. https://doi.org/http://dx.doi.org/10.1097/00002093-199912003-00017

Kimberly, W. T., Gilson, A., Rost, N. S., Rosand, J., Viswanathan, A., Smith, E. E., & Greenberg, S. M. (2009). Silent ischemic infarcts are associated with hemorrhage burden in cerebral amyloid angiopathy. *Neurology*, *72*(14), 1230–1235. https://doi.org/10.1212/01.wnl.0000345666.83318.03

Knudsen, K. A., Rosand, J., Karluk, D., & Greenberg, S. M. (2001). Clinical diagnosis of cerebral amyloid angiopathy: validation of the Boston criteria. *Neurology*, *56*(4), 537–539. https://doi.org/10.1212/WNL.56.4.537

Kumar, N. (2007). Superficial siderosis: associations and therapeutic implications. *Archives of Neurology*, *64*(4), 491–496. https://doi.org/10.1001/archneur.64.4.491

Linn, J., Halpin, A., Demaerel, P., Ruhland, J., Giese, A. D., Dichgans, M., … Greenberg, S. M. (2010). Prevalence of superficial siderosis in patients with cerebral amyloid angiopathy. *Neurology*, *74*(17), 1346–1350. https://doi.org/10.1212/WNL.0b013e3181dad605

Linn, J., Wollenweber, F. A., Lummel, N., Bochmann, K., Pfefferkorn, T., Gschwendtner, A., … Opherk, C. (2013). Superficial siderosis is a warning sign for future intracranial hemorrhage. *Journal of Neurology*, *260*(1), 176–181. https://doi.org/10.1007/s00415-012-6610-7

Lummel, N., Wollenweber, F. A., Demaerel, P., Bochmann, K., Malik, R., Opherk, C., & Linn, J. (2015). Clinical spectrum, underlying etiologies and radiological characteristics of cortical superficial siderosis. *Journal of Neurology*, *262*(6), 1455–1462. https://doi.org/10.1007/s00415-015-7736-1

Martinez-Ramirez, S., Romero, J. R., Shoamanesh, A., McKee, A. C., Van Etten, E., Pontes-Neto, O., … Viswanathan, A. (2015). Diagnostic value of lobar microbleeds in individuals without intracerebral hemorrhage. *Alzheimer's and Dementia*, *11*(12), 1480–1488. https://doi.org/10.1016/j.jalz.2015.04.009

Mesulam, M., Siddique, T., & Cohen, B. (2003). Cholinergic denervation in a pure multi-infarct state: observations on CADASIL. *Neurology*, *60*(7), 1183–1185. https://doi.org/10.1212/01.WNL.0000055927.22611.EB

Molko, N., Pappata, S., Mangin, J. F., Poupon, F., LeBihan, D., Bousser, M. G., & Chabriat, H. (2002). Monitoring disease progression in CADASIL with diffusion magnetic resonance imaging: a study with whole brain histogram analysis. *Stroke, 33*(12), 2902-2908. https://doi.org/10.1161/01.STR.0000041681.25514.22

Nandigam, R. N. K., Viswanathan, A., Delgado, P., Skehan, M. E., Smith, E. E., Rosand, J., … Dickerson, B. C. (2009). MR imaging detection of cerebral microbleeds: effect of

susceptibility-weighted imaging, section thickness, and field strength. *AJNR American Journal of Neuroradiology*, *30*(2), 338–343. https://doi.org/10.3174/ajnr.A1355

Ngandu, T., Lehtisalo, J., Solomon, A., Levälahti, E., Ahtiluoto, S., Antikainen, R., … Kivipelto, M. (2015). A 2 year multidomain intervention of diet, exercise, cognitive training, and vascular risk monitoring versus control to prevent cognitive decline in at-risk elderly people (FINGER): a randomised controlled trial. *The Lancet*, *385*(9984), 2255–2263. https://doi.org/10.1016/S0140-6736(15)60461-5

NICE, National Collaborating Centre for Mental Health (2006). Clinical Guideline 42. Dementia: Supporting People with Dementia and their Carers in Health and Social Care. *National Institute for Health and Care Excellence*.

Nitkunan, A., Barrick, T. R., Charlton, R. a., Clark, C. a., & Markus, H. S. (2008). Multimodal MRI in cerebral small vessel disease: Its relationship with cognition and sensitivity to change over time. *Stroke*, *39*(7), 1999–2005. https://doi.org/10.1161/STROKEAHA.107.507475

Nitkunan, A., Lanfranconi, S., Charlton, R. A., Barrick, T. R., & Markus, H. S. (2011). Brain atrophy and cerebral small vessel disease a prospective follow-up study. *Stroke*, *42*(1), 133–138. https://doi.org/10.1161/STROKEAHA.110.594267

Nucifora, P. G. P., Verma, R., Lee, S.-K., & Melhem, E. R. (2007). Diffusion-tensor MR imaging and tractography: exploring brain microstructure and connectivity. *Radiology*, *245*(2), 367–384. https://doi.org/10.1148/radiol.2452060445

O'Brien, J. T., Erkinjuntti, T., Reisberg, B., Roman, G., Sawada, T., Pantoni, L., … DeKosky, S. T. (2003). Vascular cognitive impairment. *The Lancet Neurology*, *2*(2), 89–98. https://doi.org/10.1016/S1474-4422(03)00305-3

O'Brien, J. T., & Thomas, A. (2015). Vascular dementia. *The Lancet*, *386*(10004), 1698–1706. https://doi.org/10.1016/S0140-6736(15)00463-8

O'Sullivan, M., Jarosz, J. M., Martin, R. J., Deasy, N., Powell, J. F., & Markus, H. S. (2001). MRI hyperintensities of the temporal lobe and external capsule in patients with CADASIL. *Neurology*, *56*(5), 628–634. https://doi.org/10.1212/WNL.56.5.628

O'Sullivan, M., Morris, R. G., Huckstep, B., Jones, D. K., Williams, S. C., & Markus, H. S. (2004). Diffusion tensor MRI correlates with executive dysfunction in patients with

ischaemic leukoaraiosis. *Journal of Neurology, Neurosurgery & Psychiatry*, *75*(3), 441–447. https://doi.org/10.1136/jnnp.2003.014910

Orgogozo, J. M., Rigaud, A. S., Stöffler, A., Möbius, H. J., & Forette, F. (2002). Efficacy and safety of memantine in patients with mild to moderate vascular dementia: A randomized, placebo-controlled trial (MMM 300). *Stroke*, *33*(7), 1834–1839. https://doi.org/10.1161/01.STR.0000020094.08790.49

Pantoni, L. (2002). Pathophysiology of Age-Related Cerebral White Matter Changes. *Cerebrovascular Diseases*, *13*(2), 7–10. https://doi.org/10.1159/000049143

Pantoni, L. (2010). Cerebral small vessel disease: from pathogenesis and clinical characteristics to therapeutic challenges. *The Lancet Neurology*, *9*(7), 689–701. https://doi.org/10.1016/S1474-4422(10)70104-6

Pantoni, L., & Garcia, J. H. (1997). Pathogenesis of Leukoaraiosis A Review. *Stroke*, *28*(3), 652–659. https://doi.org/10.1161/01.STR.28.3.652

Patel, B., & Markus, H. S. (2011). Magnetic resonance imaging in cerebral small vessel disease and its use as a surrogate disease marker. *International Journal of Stroke*, *6*(1), 47–59. https://doi.org/10.1111/j.1747-4949.2010.00552.x

Peters, N., Holtmannspotter, M., Opherk, C., Gschwendtner, A., Herzog, J., Samann, P., & Dichgans, M. (2006). Brain volume changes in CADASIL: A serial MRI study in pure subcortical ischemic vascular disease. *Neurology*, *66*(10), 1517–1522. https://doi.org/10.1212/01.wnl.0000216271.96364.50

Peters, N., Opherk, C., Bergmann, T., Castro, M., Herzog, J., & Dichgans, M. (2005). Spectrum of mutations in biopsy-proven CADASIL. *Archives of Neurology*, *62*(7), 1091-1094. https://doi.org/10.1001/archneur.62.7.1091

Poels, M., Ikram, M., van der Lught, A., Hofman, A., Niessan, W., Krestin, G., … Vernooij, M. W. (2012). Cerebral microbleeds are associated with worse cognitive function. *Neurology*, *78*(5), 326–333. https://doi.org/10.1212/WNL.0b013e3182452928

Prins, N. D., & Scheltens, P. (2015). White matter hyperintensities, cognitive impairment and dementia: an update. *Nature Reviews Neurology*, *11*(3), 157–165. https://doi.org/10.1038/nrneurol.2015.10

Qureshi, A. I., Tuhrim, S., Broderick, J. P., Batjer, H. H., Hondo, H., & Hanley, D. F. (2001). Spontaneous intracerebral hemorrhage. *The New England Journal of Medicine*, *344*(19), 1450–1460. https://doi.org/10.1056/NEJM200105103441907

Reijmer, Y. D., van Veluw, S. J., & Greenberg, S. M. (2016). Ischemic brain injury in cerebral amyloid angiopathy. *Journal of Cerebral Blood Flow & Metabolism*, *36*(1), 40–54. https://doi.org/10.1038/jcbfm.2015.88

Sachdev, P. S. (2005). White matter hyperintensities are related to physical disability and poor motor function. *Journal of Neurology, Neurosurgery & Psychiatry*, *76*(3), 362–367. https://doi.org/10.1136/jnnp.2004.042945

Schmidt, R., Ropele, S., Enzinger, C., Petrovic, K., Smith, S., Schmidt, H., … Fazekas, F. (2005). White matter lesion progression, brain atrophy, and cognitive decline: The Austrian stroke prevention study. *Annals of Neurology*, *58*(4), 610–616. https://doi.org/10.1002/ana.20630

Shoamanesh, A., Kwok, C. S., & Benavente, O. (2011). Cerebral microbleeds: histopathological correlation of neuroimaging. *Cerebrovascular Diseases, 32*(6), 528-534. https://doi.org/10.1159/000331466

Smith, E. E., & Eichler, F. (2006). Cerebral amyloid angiopathy and lobar intracerebral hemorrhage. *Archives of neurology, 63*(1), 148-151. https://doi.org/10.1001/archneur.63.1.148

Thijs, V., Lemmens, R., Schoofs, C., Görner, A., Van Damme, P., Schrooten, M., & Demaerel, P. (2010). Microbleeds and the risk of recurrent stroke. *Stroke, 41*(9), 2005-2009. https://doi.org/10.1161/STROKEAHA.110.588020

Van Dalen, J. W., van Charante, E. P. M., Caan, M. W., Scheltens, P., Majoie, C. B., Nederveen, A. J., ... & Richard, E. (2017). Effect of long-term vascular care on progression of cerebrovascular lesions: magnetic resonance imaging substudy of the PreDIVA trial (Prevention of Dementia by Intensive Vascular Care). *Stroke, 48*(7), 1842-1848. https://doi.org/10.1161/STROKEAHA.117.017207

Van Norden, A. G. W., de Laat, K. F., van Dijk, E. J., van Uden, I. W. M., van Oudheusden, L. J. B., Gons, R. A. R., … de Leeuw, F.-E. (2012). Diffusion tensor imaging and cognition in cerebral small vessel disease. *Biochimica et Biophysica Acta (BBA) - Molecular Basis of Disease*, *1822*(3), 401–407.

https://doi.org/10.1016/j.bbadis.2011.04.008

Vermeer, S. E., Longstreth, W. T., & Koudstaal, P. J. (2007). Silent brain infarcts: a systematic review. *The Lancet Neurology*, *6*(7), 611–619. https://doi.org/10.1016/S1474-4422(07)70170-9

Vernooij, M. W., van der Lugt, A., Ikram, M. A., Wielopolski, P. A., Niessen, W. J., Hofman, A., ... & Breteler, M. M. B. (2008). Prevalence and risk factors of cerebral microbleeds The Rotterdam Scan Study. *Neurology, 70*(14), 1208-1214. https://doi.org/10.1212/01.wnl.0000307750.41970.d9

Vernooij, M. W., Ikram, M. A., Hofman, A., Krestin, G. P., Breteler, M. M. B., & Van Der Lugt, A. (2009). Superficial siderosis in the general population. *Neurology*, *73*(3), 202–205. https://doi.org/10.1212/WNL.0b013e3181ae7c5e

Vinters, H. V. (1983). Cerebral amyloid angiopathy. A critical review. *Stroke*, *18*(2), 311–24. https://doi.org/10.1161/01.STR.14.6.915

Viswanathan, A., Godin, O., Jouvent, E., O'Sullivan, M., Gschwendtner, A., Peters, N., … Chabriat, H. (2010). Impact of MRI markers in subcortical vascular dementia: A multi-modal analysis in CADASIL. *Neurobiology of Aging*, *31*(9), 1629–1636. https://doi.org/10.1016/j.neurobiolaging.2008.09.001

Viswanathan, A., & Greenberg, S. M. (2011). Cerebral amyloid angiopathy in the elderly. *Annals of Neurology*, *70*(6), 871–880. https://doi.org/10.1002/ana.22516

Wahlund, L. O., Barkhof, F., Fazekas, F., Bronge, L., Augustin, M., Sjögren, M., ... & Pasquier, F. (2001). A new rating scale for age-related white matter changes applicable to MRI and CT. *Stroke, 32*(6), 1318-1322. https://doi.org/10.1161/01.STR.32.6.1318

Wardlaw, J. M., Smith, C., & Dichgans, M. (2013a). Mechanisms of sporadic cerebral small vessel disease: insights from neuroimaging. *The Lancet Neurology*, *12*(5), 483–497. https://doi.org/10.1016/S1474-4422(13)70060-7

Wardlaw, J. M., Smith, E. E., Biessels, G. J., Cordonnier, C., Fazekas, F., Frayne, R., … Dichgans, M. (2013b). Neuroimaging standards for research into small vessel disease and its contribution to ageing and neurodegeneration. *The Lancet Neurology*, *12*(8), 822–838. https://doi.org/10.1016/S1474-4422(13)70124-8

Wilkinson, D., Doody, R., Helme, R., Taubman, K., Mintzer, J., Kertesz, a, & Pratt, R. D. (2003). Donepezil in vascular dementia: a randomized, placebo-controlled study. *Neurology*, *61*(4), 479–486. https://doi.org/10.1212/01.WNL.0000078943.50032.FC

Wollenweber, F. A., Buerger, K., Mueller, C., Ertl-Wagner, B., Malik, R., Dichgans, M., … Opherk, C. (2014). Prevalence of cortical superficial siderosis in patients with cognitive impairment. *Journal of Neurology*, *261*(2), 277–282. https://doi.org/10.1007/s00415-013-7181-y

Yates, P. A., Villemagne, V. L., Ellis, K. A., Desmond, P. M., Masters, C. L., & Rowe, C. C. (2014). Cerebral microbleeds: a review of clinical, genetic, and neuroimaging associations. *Frontiers in Neurology, 4*, 205. https://doi.org/10.3389/fneur.2013.00205

PUBLISHED STUDIES
Studies on individual research questions

2.1. Study1: A Novel Imaging Marker for Small Vessel Disease Based on Skeletonization of White Matter Tracts and Diffusion Histograms

Ebru Baykara[1], Benno Gesierich[1], Ruth Adam[1], Anil Man Tuladhar[2], J. Matthijs Biesbroek[3], Huiberdina L. Koek[4], Stefan Ropele[5], Eric Jouvent[6,7,8], Alzheimer's Disease Neuroimaging Initiative, Hugues Chabriat[6,7,8], Birgit Ertl-Wagner[9], Michael Ewers[1], Reinhold Schmidt[5], Frank-Erik de Leeuw[2], Geert Jan Biessels[3], Martin Dichgans[1,10,11], and Marco Duering[1]

[1]Institute for Stroke and Dementia Research, Klinikum der Universität München, Ludwig-Maximilians-University LMU, Munich, Germany;
[2]Radboud University Medical Center, Donders Institute for Brain, Cognition, and Behavior, Department of Neurology, Nijmegen, the Netherlands;
[3]Department of Neurology, Brain Center Rudolf Magnus, University Medical Center Utrecht, Utrecht, the Netherlands;
[4]Department of Geriatrics, University Medical Center Utrecht, Utrecht, the Netherlands;
[5]Department of Neurology, Medical University of Graz, Graz, Austria;
[6]Université Paris Diderot, Sorbonne Paris Cité, UMR-S 1161 National Institute for Health and Medical Research (INSERM), Paris, France;
[7]Departement Hospitalo-Universitaire NeuroVasc Sorbonne Paris Cité, Paris, France;
[8]Department of Neurology, Lariboisière Hospital, Assistance Publique - Hôpitaux de Paris, Paris, France;
[9]Institute of Clinical Radiology, Klinikum der Universität München, Ludwig-Maximilians-University LMU, Munich, Germany;
[10]Munich Cluster for Systems Neurology (SyNergy), Munich, Germany; and
[11]German Center for Neurodegenerative Diseases (DZNE), Munich, Germany.
A complete listing of Alzheimer's Disease Neuroimaging Initiative investigators can be found at: http://adni.loni.usc.edu/wp-content/uploads/how_to_apply/ADNI_Acknowledgement_List.pdf

Baykara, E. et al., (2016). A novel imaging marker for small vessel disease based on skeletonization of white matter tracts and diffusion histograms. *Annals of Neurology*, *80(4),* 581-92. doi: 10.1002/ana.24758.

2.1.1. Abstract

Objective: To establish a fully-automated, robust imaging marker for cerebral small vessel disease (SVD) and related cognitive impairment, that is easy to implement, reflects disease burden, and is strongly associated with processing speed, the predominantly affected cognitive domain in SVD.

Methods: We developed a novel MRI marker based on diffusion tensor imaging, skeletonization of white matter tracts, and histogram analysis. The marker (peak width of skeletonized mean diffusivity, PSMD) was assessed along with conventional SVD imaging markers. We first evaluated associations with processing speed in patients with genetically defined SVD (n=113). Next, we validated our findings in independent samples of inherited SVD (n=57), sporadic SVD (n=444), and in memory clinic patients with SVD (n=105). The new marker was further applied to healthy controls (n=241) and to patients with Alzheimer's disease (n=153). We further conducted a longitudinal analysis and inter-scanner reproducibility study.

Results: PSMD was associated with processing speed in all study samples with SVD (p-values between 2.8×10^{-3} and 1.8×10^{-10}). PSMD explained most of the variance in processing speed (R^2 ranging from 8.8% to 46%) and consistently outperformed conventional imaging markers (white matter hyperintensity volume, lacune volume, and brain volume) in multiple regression analyses. Increases in PSMD were linked to vascular but not to neurodegenerative disease. In longitudinal analysis, PSMD captured SVD progression better than other imaging markers.

Interpretation: PSMD is a new, fully automated, and robust imaging marker for SVD. PSMD can easily be applied to large samples and may be of great utility for both research studies and clinical use.

2.1.2. Introduction

Cerebral small vessel disease (SVD) represents a major cause of vascular cognitive impairment (VCI) and dementia, either by its own or in combination with neurodegenerative pathology (Pantoni, 2010). Progress in understanding and managing SVD has been relatively slow. This in part relates to the lack of a good disease marker that is quantitative, robust, reflects disease burden, and can easily be applied to a large number of subjects.

Previous studies have suggested a wide range of mostly MRI-based markers for SVD and VCI. The most commonly used markers are white matter hyperintensity (WMH) and lacune volumes (Wardlaw, Smith, Biessels, et al., 2013). Yet, both markers have clear limitations. First, lesion quantification is labor-intensive and subject to bias because of errors in lesion classification and the requirement for manual corrections (Wardlaw, Valdés Hernández, & Muñoz-Maniega, 2015). Second, associations with clinical symptoms, such as cognitive deficits are typically weak (Nitkunan et al., 2008; Patel & Markus, 2011). Stronger associations have been reported for brain volume (Duering et al., 2011; Nitkunan et al., 2008; Viswanathan et al., 2010). However, alterations in brain volume are relatively unspecific and generally considered a marker for neurodegenerative pathology (Frisoni et al., 2010). Also, automated volumetric analysis of diseased brains is methodologically challenging because of altered tissue contrast (De Guio et al., 2014; O'Sullivan et al., 2008). Hence, there is great demand for better markers of SVD burden (Charidimou & Werring, 2012; Smith, Schneider, Wardlaw, & Greenberg, 2012; Wardlaw, Smith, Biessels, et al., 2013).

Diffusion tensor imaging (DTI) is a sensitive technique that allows quantifying microstructural tissue alterations (Nucifora et al., 2007), which can be invisible on conventional MRI. The typical pattern of diffusion change in SVD is a reduction in directionality, as captured by fractional anisotropy (FA), and a prominent increase in the magnitude of diffusion, as captured by mean diffusivity (MD). Previous studies suggested that these DTI metrics are superior to conventional imaging markers in assessing disease burden in SVD (Nitkunan et al., 2008; Tuladhar et al., 2015; van Norden, de Laat, et al., 2012). However, there are obstacles to the wider application of DTI measures, in particular, the need for extensive data post-processing such as the removal of prominent cerebrospinal fluid (CSF) signal from MD images.

The aim of this study was to develop a new imaging marker for disease burden in SVD that can be used in clinical routine and readily applied to large samples. We requested that this marker should reflect the underlying disease (SVD) and correlate with clinical deficits typically seen in these patients. We further reasoned that the marker should be robust, fully automated, and easy to implement. To this end, we combined two processing techniques for DTI data: skeletonization and histogram analysis. Skeletonization focuses the analysis of MD on the main fiber tracts, thereby largely eliminating CSF contamination. Whole-brain histogram analysis is particularly appropriate when dealing with diffuse diseases and when quantifying total disease burden (Tofts, Davies, & Dehmeshki, 2003).

We first established our new imaging marker, peak width of skeletonized mean diffusivity (PSMD), in patients with CADASIL (Cerebral Autosomal-Dominant Arteriopathy with Subcortical Infarcts and Leukoencephalopathy), a genetically defined form of severe SVD. We analyzed the relationship of this marker with processing speed since speed has emerged as the most prominently affected cognitive domain in SVD. Next, we validated our results in an independent sample of CADASIL patients. We then evaluated two samples comprising patients with sporadic SVD. In each sample, we compared PSMD with conventional SVD markers. We also applied the novel marker to healthy controls and patients with Alzheimer's disease (AD) pathology (Fig 1). Finally, we addressed the utility of the new marker in multicenter trials through sample size estimations and assessment of inter-scanner reproducibility.

2.1.3. Subjects and methods

Subjects, MRI acquisition, and neuropsychological testing

All studies used in this analysis were approved by the ethics committees of the respective institutions. Written informed consent was obtained from all subjects. Characteristics of the study samples are provided in Tables 1 and 2.

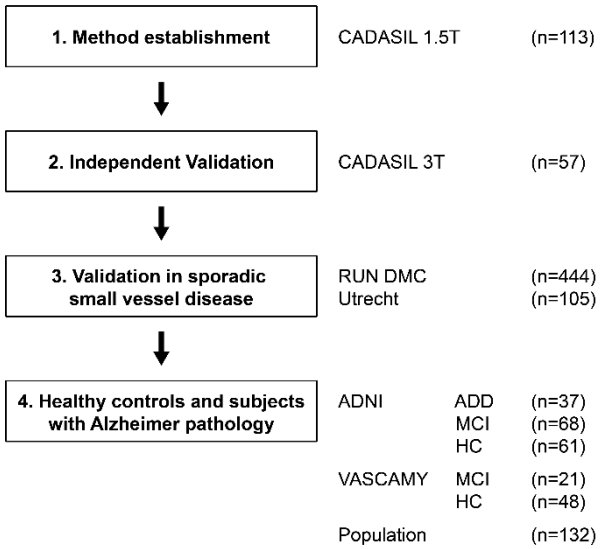

Figure 1. Study design. The new imaging marker peak width of skeletonized MD (PSMD) was first established in a large CADASIL dataset with MR imaging at 1.5T. Independent validation was performed in a new CADASIL sample scanned at 3T. In a third step the marker was applied to samples with sporadic small vessel disease (RUN DMC and Utrecht). Lastly, the marker was evaluated in healthy subjects (HC) as well as samples with predominant Alzheimer pathology (MCI and AD dementia, ADD). Numbers indicate subjects with usable DTI data in the samples.

CADASIL exploratory sample

The novel DTI-based marker was developed in an exploratory sample of 117 patients with CADASIL from a previous, prospective study (Duering, et al., 2013). The diagnosis was confirmed either by genetic testing or skin biopsy. Four patients were excluded due to insufficient quality of the DTI images. For the regression analysis on processing speed additional nine subjects were excluded because of missing neuropsychological data. Therefore, the final sample for regression analyses consisted of 104 patients.

MRI scans were performed on a 1.5T GE Healthcare Signa scanner (Solingen, Germany). Acquisition parameters are presented in Supplementary Table e-1.

Neuropsychological testing was performed on the previous or the same day as the MRI examination. Trail Making Test (TMT) matrix A and B were used to create a compound processing speed score. Raw test scores were transformed into age- and education-corrected z-scores based on values from healthy subjects (Tombaugh, 2004).

Longitudinal data (follow-up at 18 months) were available for 58 patients.

CADASIL validation sample (VASCAMY study)

A total of 57 patients with CADASIL from the ongoing, prospective VASCAMY (Vascular and amyloid predictors of neurodegeneration and cognitive decline in non-demented subjects) study were included in the validation sample. Again, the diagnosis was confirmed either by genetic testing or skin biopsy. From the same study we also included 69 non-CADASIL subjects: 21 diagnosed with (mostly amnestic) mild cognitive impairment and 48 healthy controls.

MRI scans were performed on a 3T Siemens Magnetom Verio scanner (Erlangen, Germany). For inter-scanner reproducibility analysis, 7 CADASIL patients from the VASCAMY study were scanned back-to-back on both the 3T scanner and a 1.5T Siemens Magnetom Aera scanner. Acquisition parameters are presented in Table e-1.

Neuropsychological testing was performed on the previous or the same day as the MRI examination. Similar to the exploratory sample, age- and education-corrected TMT A and B z-scores were used to create a compound processing speed score.

Sporadic small vessel disease sample (RUN DMC study)

444 subjects from the RUN DMC (Radboud University Nijmegen Diffusion tensor and Magnetic resonance imaging Cohort) study (Norden et al., 2011) were included. The processing speed scores could not be calculated for five subjects because of missing neuropsychological data. Furthermore, 3 outliers were excluded from the regression analyses (see section *Statistical analysis*) and the final sample for regression analysis consisted of 436 subjects.

MRI scans were performed on a 1.5T Siemens Magnetom Sonata scanner. Acquisition parameters are presented in Table e-1.

Neuropsychological testing was performed within 3 weeks before the scanning. The 1-letter subtask of the Paper-Pencil Memory Scanning Task and the Letter-Digit Substitution Task were used to create a compound processing speed score. Raw test scores were transformed into age- and education-corrected z-scores based on values from healthy subjects (van der Elst et al., 2006; 2007).

Memory clinic patients with small vessel disease (Utrecht)

133 subjects from the Memory Clinic cohort of the Utrecht Vascular Cognitive Impairment Study Group were included. Recruitment and data collection was done according to the multicenter Dutch Parelsnoer Institute Neurodegenerative diseases protocol (Aalten et al., 2014). 23 subjects had to be excluded due to motion slice artifacts in the DTI data. 5 subjects had missing structural MRI data (T1, FLAIR or both) and were therefore not included in further analyses. Of the remaining 105 patients, 10 presented with subjective cognitive complaints, 43 with mild cognitive impairment (according to the Peterson criteria; Petersen, 2004) and 52 with dementia. In order to focus on patients with SVD within the memory clinic sample, we performed a pre-specified subgroup analysis: Subgroups were pre-defined according to the WMH load by splitting at the median normalized WMH volume. Subgroups consisted of 52 subjects with low WMH load and 53 with high WMH load. Three subjects from the low WMH and 6 subjects from the high WMH group had to be excluded from regression analyses because of missing cognitive data.

MRI scans were performed on a Philips Intera 3T scanner (Best, The Netherlands). Acquisition parameters are presented in Table e-1.

Neuropsychological testing was performed on the same day as the MRI examination. Similar to the CADASIL samples, age- and education-corrected TMT A and B z-scores were used to create a compound processing speed score (mean of both Z-scores).

Alzheimer's Disease Neuroimaging Initiative Study (ADNI)

The Alzheimer's Disease Neuroimaging Initiative was launched in 2003 as a public-private partnership, led by Principal Investigator Michael W. Weiner, MD (for up-to-date information, see www.adni-info.org). 185 subjects from the ADNI database (http://adni.loni.usc.edu/) (from 17 centers with the same DTI protocol, ADNIGO and ADNI2 phases) were included in the current study. 19 subjects were excluded due to either missing diagnosis, missing MRI data or motion artifacts in the DTI data. The final sample consisted of 166 subjects, of whom 61 were healthy controls, 68 amnestic mild cognitive impairment (MCI) subjects and 37 AD dementia patients (diagnosis according to the NINCDS-ADRDA criteria for probable AD as outlined in the ADNI protocol).

MRI scans were performed on 3T GE Healthcare scanners (Signa HDxt and Discovery MR750). Acquisition parameters are presented in Table e-1.

Austrian Stroke Prevention Family Study (ASPFS)

135 community-dwelling, healthy subjects with DTI data were included from the Austrian Stroke Prevention Family Study (ASPFS – Department of Neurology, Medical University Graz) (Ghadery et al., 2015). Three subjects were excluded due to insufficient data quality of the DTI images. The final sample consisted of 132 subjects.

MRI scans were performed on a 3T Siemens Magnetom Tim Trio scanner. Acquisition parameters are presented in Table e-1.

MRI processing

Diffusion tensor imaging

After a quick (maximum = 15 seconds) visual inspection to exclude the presence of major artifacts, diffusion-weighted images were corrected for eddy current induced distortions and subject motion with the eddy_correct tool of the Functional Magnetic Resonance Imaging of the Brain (FMRIB) software library (FSL; v5.0) (Smith et al., 2004). In RUN DMC, diffusion data were pre-processed using the in-house-developed iteratively reweighted-least-squares algorithm 'PATCH' (Zwiers, 2010). After brain tissue extraction using BET (FSL), diffusion tensors and scalar diffusion parameters (i.e. FA and MD) were calculated using DTIFIT (FSL).

Peak width of skeletonized mean diffusivity (PSMD)

Fully automated calculation of the new marker comprised 2 steps: Skeletonization of DTI data and histogram analysis (Fig 2). All study samples were processed through the same pipeline. First, DTI data were skeletonized using the Tract-Based Spatial Statistics procedure (TBSS) (Smith, Jenkinson, & Johansen-Berg, 2006), part of FSL. For this purpose, all subjects' FA data were aligned into a common space using the nonlinear registration tool FNIRT and the standard space FMRIB 1mm FA template. Each subject's FA data was then projected onto the skeleton, which was derived from the standard space template thresholded at an FA value of 0.2. Finally, MD images were projected onto the skeleton, using the FA-derived projection parameters. The final MD skeletons were further masked with the template skeleton thresholded at an FA value of 0.3 in order to avoid contamination of the skeleton through CSF partial volume effects. For the same reason, regions of the skeleton

directly adjacent to the ventricles, such as the fornix, were removed from further analysis by a custom-made mask. The same template skeleton and mask were used for each study sample.

The new marker, “peak width of skeletonized MD” (PSMD) was calculated as the difference between the 95th and 5th percentiles of the voxel-based MD values within the skeleton (see Fig 2). We compared PSMD to established MD parameters (mean, median, peak height, full width at half maximum) in the exploratory CADASIL sample: PSMD showed the strongest association with processing speed scores and was therefore used for all subsequent analyses in all study samples.

A shell script for the calculation of PSMD is available at http://www.psmd-marker.com/. The total calculation for one subject (from DTI raw data) takes approximately 12 minutes on a standard desktop computer. All processing steps (including pre-processing) are included in the shell script. No human intervention (e.g. visual inspection or manual edits) is needed during or after the processing pipeline.

For comparison, we also calculated whole brain MD peak height, an established histogram measure for non-skeletonized data. First, CSF was removed by a conventional method (i.e. intensity thresholding with a value of 0.0025). Next, the peak height of the histogram was estimated using the density function in R (v3.1.2, R Core Team, 2014) and normalized by the total number of voxels in the histogram.

Normalized brain volume

In each sample, brain parenchymal fraction (BPF; i.e. normalized brain volume) was calculated by dividing the whole brain volume by intracranial cavity volume.

For the CADASIL exploratory sample and the RUN DMC study the brain volume calculation procedure has already been described (Duering et al., 2011; Tuladhar et al., 2015). Due to uncorrectable failure in either brain or intracranial segmentation we could not calculate BPF for 2 CADASIL subjects.

In the VASCAMY study, native space T1 and T2 images were segmented into tissue probability maps using the Statistical Parametric Mapping (SPM) toolbox (v12; Wellcome Department of Cognitive Neurology, London, UK; http://www.fil.ion.ucl.ac.uk/spm). For whole brain volume, T1 segmented grey matter and white matter tissue maps; for the

intracranial volume, T2 segmented grey matter, white matter, and CSF) were combined, thresholded at 20 % and binarized. Manual editing was performed when necessary.

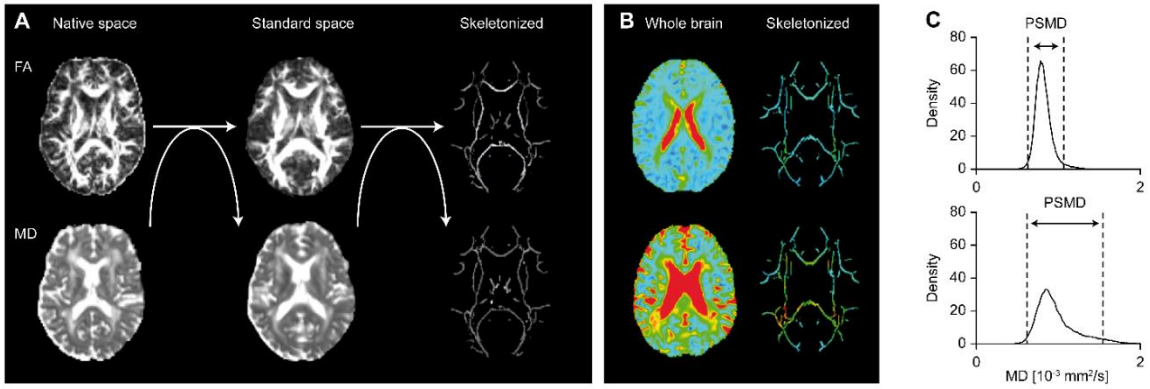

Figure 2. Procedure for marker calculation: Skeletonization and histogram analysis.

(A) Illustration of the automated skeletonization procedure. Individual FA images are normalized to standard space and projected onto the skeleton template. Next, the transformation and skeleton projection parameters are applied to the MD images. (B) Examples of MD maps from two CADASIL subjects (upper and lower panel) projected onto the standard skeleton. (C) Histogram analysis of the same MD data as in B. PSMD is calculated as the difference between the 95th and 5th percentiles.

Table 1. Characteristics of study samples with predominant vascular disease

	CADASIL exploratory, n=113	CADASIL validation (VASCAMY), n=57	Sporadic SVD (RUN DMC), n=444	Memory clinic patients with SVD (Utrecht), n=105
Demographic characteristics				
Age, yr, mean (SD) [min, max]	49.1 (9.5) [22.9, 72.8]	53.4 (10.7) [29.0, 72.0]	65.3 (8.9) [49.6, 85.5]	74.9 (8.3) [50.0, 92.0]
Education, yr, mean (SD) [min, max]	10.5 (2.2) [9, 16]	14 (2.7) [10, 20]	11 (3.6) [4, 19]	12.2 (2.7) [4, 17]
Female, No. {%}	61 {54.0}	19 {33.3}	201 {45.3}	51 {48.6}
Vascular risk factors, No. {%}				
Current smoker	28 {24.8}	11 {19.3}	69 {15.5}	10 {9.5}
Past smoker	39 {34.5}	24 {42.1}	239 {53.8}	57 {54.3}
Hypertension	26 {23.0}	13 {22.8}	320 {72.1}	97 {92.4}
Hypercholesterolemia	36 {31.9}	24 {42.1}	194 {43.7}	64 {61.0}
Diabetes	0 {0.0}	0 {0.0}	61 {13.7}	29 {27.6}
Cognitive scores				
TMT-A,[a] median (IQR) [min, max]	-0.85 (2.64) [-22.22, 1.39]	-0.50 (1.61) [-13.24, 1.34]	-	-1.29 (3.03) [-13.05, 1.02]
TMT-B,[a] median (IQR) [min, max]	-2.14 (4.60) [-16.38, 1.67]	-0.48 (3.05) [-11.59, 1.72]	-	-1.73 (3.05) [-22.11, 1.51]
1-letter P&P MST,[a] median (IQR) [min, max]	-	-	-2.91 (2.71) [-17.97, 1.45]	-
LDST,[a] median (IQR) [min, max]	-	-	-0.38 (2.15) [-3.74, 4.47]	-
Speed score,[a] median (IQR) [min, max]	-1.56 (2.80) [-17.44, 1.24]	-0.56 (2.33) [-12.42, 1.16]	-1.67 (2.17) [-10.20, 2.96]	-1.73 (2.60) [-11.52, 1.13]
MMSE, median (IQR) [min, max]	29 (3) [15, 30]	30 (1) [22, 30]	29 (2) [22, 30]	26 (4) [20, 30]
Imaging characteristics				
PSMD, 10^{-4} mm^2/s, median (IQR) [min, max]	5.43 (2.92) [2.82, 10.87]	5.47 (2.69) [2.63, 9.47]	3.28 (0.87) [2.30, 7.95]	4.24 (1.05) [2.82, 8.72]
Normalized WMHV, %, median (IQR) [min, max]	9.81 (8.80) [0.06, 30.99]	7.38 (7.53) [0.09, 22.84]	0.59 (1.23) [0.05, 14.03]	1.12 (2.58) [0, 7.70]
Normalized LV, %, median (IQR) [min, max]	0.0093 (0.0315) [0, 0.2118]	0.0240 (0.0639) [0, 0.2477]	0 (0) [0, 0.1027]	0 (0) [0, 0.0577]
BPF, median (IQR) [min, max]	0.836 (0.068) [0.655, 0.935]	0.784 (0.069) [0.699, 0.872]	0.654 (0.077) [0.499, 0.809]	0.621 (0.055) [0.528, 0.759]

[a]age & education adjusted z-scores. BPF=brain parenchymal fraction; IQR=interquartile range; LDST=letter digit substitution test; LV=lacune volume; MMSE=mini mental state examination; P&P MST=paper pencil memory scanning test; PSMD=peak width of skeletonized mean diffusivity; SD=standard deviation; TMT=trail making test; WMHV=white matter hyperintensity volume.

Table 2. Characteristics of healthy controls and patients with AD pathology

	HC (VASCAMY), n=48	MCI (VASCAMY), n=21	HC (ADNI), n=61	MCI (ADNI), n=68	ADD (ADNI), n=37	Population (ASPFS), n=132
Demographic characteristics						
Age, yr, mean (SD) [min, max]	71.5 (6.3) [60, 84]	76.5 (4.4) [70, 87]	72.9 (5.7) [60.4, 87]	74.7 (8.1) [48.7, 88.6]	74 (8.2) [55.9,90.2]	66.9 (11.4) [40, 85]
Education, yr, mean (SD) [min, max]	14 (3.1) [8, 20]	14 (3.7) [7, 20]	16.5 (2.8) [12, 20]	15.9 (2.7) [11, 20]	15 (2.8) [11, 20]	11.4 (2.8) [9, 18]
Female, No. {%}	30 {62.5}	11 {52.4}	37 {60.7}	24 {35.3}	12 {32.4}	81 {61.4}
Global cognitive score						
MMSE, median (IQR) [min, max]	30 (1) [27, 30]	27 (3) [22, 30]	29 (2) [24, 30]	27 (3) [23, 30]	23 (3) [15, 27]	28 (1) [23, 30]
Imaging characteristics						
PSMD, $10^{-4}mm^2/s$, median (IQR) [min, max]	3.05 (0.47) [2.58, 4.96]	3.33 (0.62) [2.72, 5.37]	3.02 (0.72) [2.23,6.85]	3.20 (0.88) [2.35, 5.03]	3.47 (0.96) [2.59, 5.03]	3.05 (0.72) [2.16, 6.76]

ADD=Alzheimer's disease dementia; ASPFS=Austrian Stroke Prevention Family Study (comprising healthy elderly from the population); HC=healthy control; IQR=interquartile range; MCI=mild cognitive impairment; MMSE=mini mental state examination; PSMD=peak width of skeletonized mean diffusivity; SD=standard deviation.

In the Utrecht study, native space T1 images and T2 images were segmented into tissue probability maps using SPM. For whole brain volume, T1 segmented grey matter and white matter tissue maps were combined, thresholded at 30 %, and binarized. Intracranial volume was calculated using the BET (brain extraction) tool (FSL) on T2 images and the resulting masks were manually edited if necessary.

Subcortical lesion volumes

We used the STRIVE (Wardlaw et al., 2013b) criteria to define and identify white matter hyperintensities (WMH) and lacunes of presumed vascular origin. Detection and segmentation procedures have already been described for the CADASIL exploratory sample, the RUN DMC study, and the ADNI study (Decarli, Maillard, & Fletcher, 2013; Duering et al., 2011; Tuladhar et al., 2015). Normalized WMH and lacune volumes for each sample were calculated by dividing through brain volume. For WMH volume in the CADASIL validation (VASCAMY study) and Utrecht samples, bias-corrected 3-dimensional (3D) FLAIR images

were first segmented into 3 tissue probability maps using FAST tool from FSL. Next, WMHs were separated from CSF, which is located in the same tissue probability map, by histogram segmentation based on the Otsu method (Otsu, 1979). The WMH segmentations were then manually edited and cleaned from misclassified artifacts using a custom 3D editing tool.

To determine the lacune volume in the CADASIL validation and Utrecht samples, we used a seed-growing algorithm, implemented via an in-house software tool. After manually placing a seed voxel into a lacune on the 3D T1 image by an experienced rater, the tool tests all neighboring voxels for inclusion and repeats testing until no new voxels can be added. The inclusion criterion was the absolute intensity of the tested voxel and its intensity difference to the seed voxel. All cavities smaller than 3mm were ignored to exclude perivascular spaces.

Cerebral microbleeds

Using the STRIVE (Wardlaw et al., 2013) criteria, cerebral microbleeds were identified and counted on T2*-weighted gradient echo images by trained raters.

Statistical analysis

All statistical analyses were performed in R (v3.1.2; R Core Team, 2014). The association between MRI parameters (PSMD, normalized WMH volume, normalized lacune volume, BPF, and microbleed count), age, sex, and the processing speed scores was evaluated by linear regression. The distributions of speed scores were tested for normality in each sample with the Shapiro-Wilk test and scores were log transformed in case of non-normal distribution. In order to ensure that the regression results were not driven by outliers, they were identified with the Bonferroni outlier test (car R package, v2.0-25; Fox & Weisberg, 2011) and excluded from regression analyses (only 3 subjects from the RUN DMC sample).

To identify the imaging marker with the highest relative importance, we included all markers into multiple linear regression models and applied a model decomposition method described by Lindeman, Merenda, and Gold (1980), as implemented in the relaimpo R package (v2.2-2; Grömping, 2006). Additionally, we used stepwise backward regression with MRI parameters, age, and sex to identify independent associations with processing speed. The Akaike Information Criterion (AIC) was used to select the model with the best fit (minimized AIC value). All R^2 values reported are adjusted R^2 values. For group comparisons

of PSMD across different clinical samples (within studies) we used the Wilcoxon rank sum test. To correct for multiple comparisons, Bonferroni-corrected p-values are reported for group comparisons. The sample size estimates were calculated on the longitudinal change of variables using the G*Power tool (Faul, Erdfelder, Lang, & Buchner, 2007) (difference between two independent means, two-tailed, type I error rate 0.05, power 0.80). We used the raw change between baseline and follow-up data and hypothetical treatment effects of 10%, 20%, and 30%. Inter-scanner reproducibility was assessed by the intraclass correlation coefficient (ICC) as implemented in R.

2.1.4. Results

Demographic, clinical, and MRI characteristics of the study samples with SVD are presented in Table 1. Details on study samples with healthy controls and subjects with AD diagnosis are presented in Table 2.

Exploratory analysis in CADASIL patients

Linear regression (Supplementary Table e-2) revealed PSMD to have the strongest association with processing speed scores (Fig 3A, upper panel). Speed scores were further significantly associated with all other imaging markers and age (Table e-2). For comparison, we added an established DTI histogram marker (whole brain MD peak height), which explained less variance than PSMD (Table e-2).

Analysis of the relative importance of the regressors showed that PSMD contributed most to the multiple regression model (Fig 3A, lower panel). To determine the best model, we further conducted a backward stepwise regression. PSMD and the normalized volumes of both WMH and lacunes were retained in the final model (Table e-2).

Validation in independent samples

In the independent CADASIL validation sample, linear regression (Table e-2) revealed a strong association between PSMD and speed scores (Fig 3B, upper panel). Speed scores were further significantly associated with microbleed count, normalized lacune volume, and age (Table e-2). Importantly, PSMD contributed most to the regression model (Fig 3B, lower panel). For further exploration, we again conducted backward stepwise regression: PSMD and normalized lacune volume were retained in the final model (Table e-2).

To validate our findings in the more common, sporadic form of SVD, we next analyzed data from the RUN DMC study. Linear regression (Table e-2) showed a significant association between PSMD and speed scores (Fig 3C, upper panel). Speed scores were also significantly associated with all other imaging markers, age and sex (Table e-2). Again, PSMD contributed most to the multiple regression model (Fig 3C, lower panel). Further exploratory backward stepwise regression resulted in a final model that included only PSMD (Table e-2).

We next extended our findings to sporadic SVD in a memory clinic setting (Utrecht study). None of the linear regression analyses with the MRI markers (PSMD, normalized WMH volume, lacune volume, BPF, and microbleed count) showed a significant association with the speed scores (not shown) within the entire memory clinic sample. In subjects with prominent vascular disease as determined by a WMH load above the median value (high WMH subgroup, n=53), we found a significant association (Table e-2) between PSMD and speed scores (Fig 3D, upper panel). Speed scores were also significantly associated with age (Table e-2). Focusing on the low WMH load group (n=52), the only imaging variable that was significantly associated with speed scores was BPF (p=0.023, R^2=0.09). Importantly, PSMD contributed most to the multiple regression model (Fig 3D, lower panel). Further exploratory backward stepwise regression resulted in a final model that included PSMD and age (Table e-2).

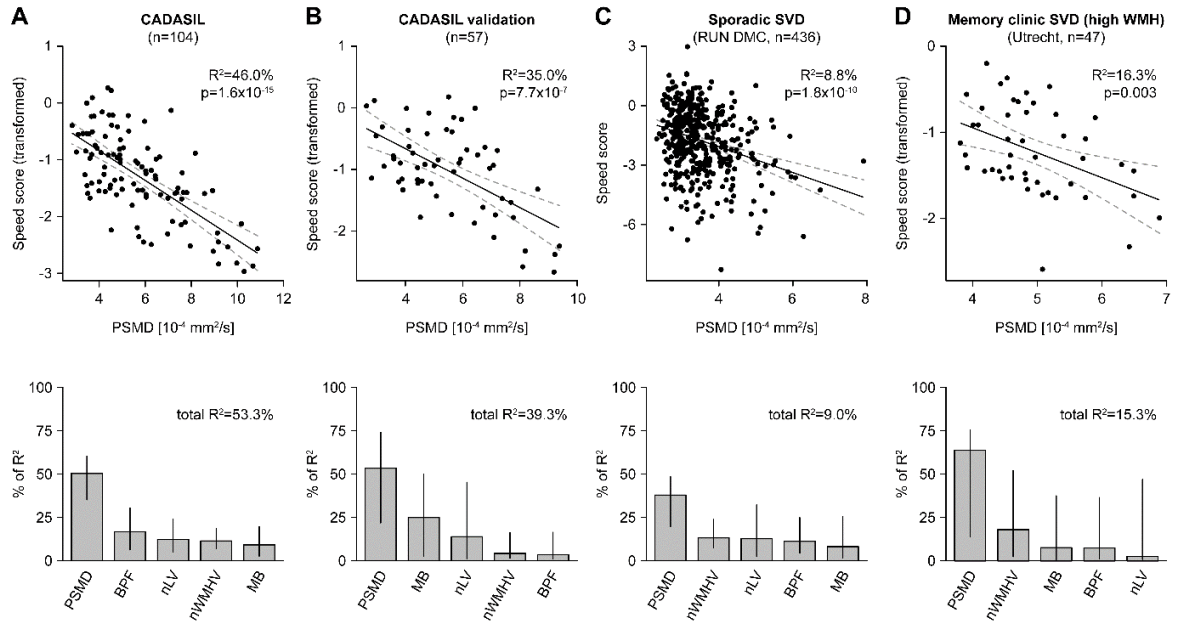

Figure 3. Association between imaging markers and processing speed performance in SVD. Upper panels: Simple linear regression between PSMD and processing speed scores in the exploratory CADASIL sample (A), the CADASIL validation sample (B), the sporadic SVD sample (RUN DMC) (C) and the memory clinic patients with SVD (Utrecht) (D). Dashed lines indicate 95% confidence intervals for the regression. Lower panels depict the contribution of each regressor (PSMD, normalized WMH volume, lacune volume, BPF, and microbleed count) to the multiple regression models as estimated by the Lindeman-Merenda-Gold method. Note that in all cases PSMD contributes most to the models. Lines represent 95% confidence intervals after bootstrapping. BPF=brain parenchymal fraction, nLV=normalized lacune volume, nWMHV=normalized white matter hyperintensity volume.

Comparison with healthy controls and subjects with Alzheimer pathology

Figure 4 demonstrates that patient samples with high SVD burden (CADASIL, RUN DMC, Utrecht) had higher PSMD compared with healthy controls and AD patients (MCI and AD dementia). Moreover, PSMD increased with higher WMH load. Focusing on the ADNI sample, there was no difference between healthy controls (PSMD median = 3.020 x 10^{-4} mm^2/s) and MCI patients with low WMH load (median = 2.935 x 10^{-4} mm^2/s, W = 903, p = 1) or AD dementia patients with low WMH load (median = 3.415 x 10^{-4} mm^2/s, W = 477, p = 1). Also, healthy controls had comparable PSMD across studies: VASCAMY (median = 3.045 x 10^{-4} mm^2/s), ADNI (median = 3.020 x 10^{-4} mm^2/s), population sample (ASPFS, median = 3.045 x 10^{-4} mm^2/s).

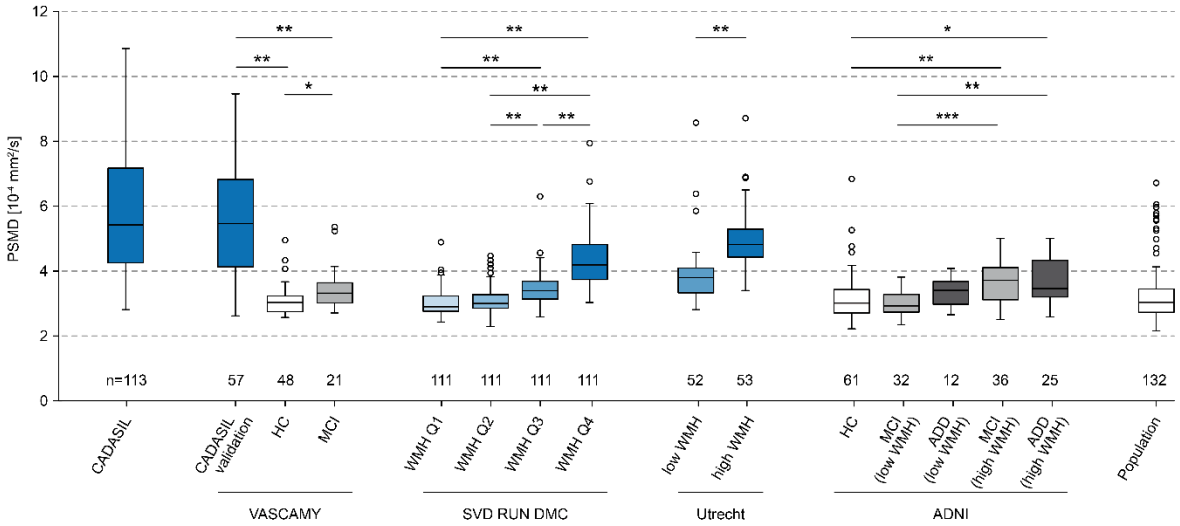

Figure 4. PSMD in subjects with SVD, healthy controls, and subjects with Alzheimer's disease. PSMD is presented across samples: CADASIL, sporadic SVD (RUN DMC, Utrecht), MCI (VASCAMY and ADNI), and AD dementia (ADNI). RUN DMC, Utrecht, and ADNI samples were split into subgroups based on the volume of white matter hyperintensities (according to median split or quartiles, Q=quartile). Group comparisons were calculated between subgroups within studies: $*p < 0.05$, $**p < 0.01$, $***p < 0.001$ (Wilcoxon rank sum tests after Bonferroni correction). ADD=Alzheimer's disease dementia, HC=healthy controls, MCI=mild cognitive impairment, SVD=small vessel disease. Samples selected on the basis of SVD pathology are indicated in blue. Samples selected on the basis of AD-typical cognitive deficits are indicated in grey.

There was no significant association between PSMD and processing speed in any of the non-SVD samples (p-values ranging between 0.24 and 0.79).

Table 3. Sample size estimation for a hypothetical clinical trial of 1.5 years duration

	Treatment effect size		
	30%	**20%**	**10%**
PSMD	96	216	859
Whole brain MD peak height	183	410	1636
Normalized WMH volume	258	580	2315
BPF	4511	10149	40592
Speed score	5387	12119	48471
Normalized Lacune volume	11354	25545	102176

BPF=brain parenchymal fraction; MD=mean diffusivity; PSMD=peak width of skeletonized mean diffusivity; WMHV=white matter hyperintensity.

2.1.5. Discussion

Our study establishes a novel imaging marker for SVD. This marker combines DTI, skeletonization of white matter tracts, and the analysis of MD histograms. Calculation of this marker is fully automated, fast, and robust, thus fulfilling the requirements for routine use and the application to large samples. PSMD explained a substantial proportion of variance in processing speed, the predominantly affected cognitive domain in SVD, and consistently outperformed other imaging makers for SVD. We could validate our findings in independent samples of SVD. We further found this marker to be linked to small vessel pathology but not to neurodegenerative pathology. Finally, PSMD showed the smallest sample size estimate in the longitudinal analysis and the highest inter-scanner reproducibility. We thus consider PSMD to be of great value for research studies and potentially also for use in clinical routine and trials.

A major finding of our study is the strong association between PSMD and deficits in processing speed across all study samples including patients with genetically defined SVD, patients with sporadic SVD, and memory clinic patients with high WMH burden. The association was strongest for patients with inherited SVD, who on average were the most severely affected group as judged by the normalized volume of WMH, the normalized volume of lacunes, and PSMD. While the association was weaker for patients with sporadic SVD, PSMD consistently showed the strongest contribution to processing speed impairment when compared with other imaging markers. Importantly, as judged by stepwise regression analyses, PSMD was the only imaging marker showing an independent association with processing speed in every SVD sample.

Methodological challenges in quantifying disease burden have been a major roadblock to research on SVD and related cognitive impairment. The superior performance of PSMD over conventional MRI markers results from the combination of DTI, skeletonization of white matter tracts, and histogram analysis. DTI is a quantitative method that is particularly well suited to characterize microstructural integrity. In contrast, lesion volumes (WMH or lacunes) rely on binary segmentations of non-quantitative images. Hence, lesion volumes disregard gradual differences in tissue damage found in SVD (Maillard et al., 2011). In addition, DTI measures are more sensitive in capturing SVD-related changes as evidenced by altered DTI measures in white matter appearing normal on conventional imaging (De Groot

et al., 2013; van Norden et al., 2012a). Previous studies found DTI parameters to correlate with cognitive performance both cross-sectionally (Lawrence et al., 2013; Tuladhar et al., 2015; van Norden et al., 2012a) and over time (Jokinen et al., 2013; Nitkunan et al., 2008), and in most studies DTI measures were found to correlate with cognitive scores independent of conventional SVD markers. However, one study found DTI to add little on top of brain and lesion volumes (van Norden et al., 2012b). Histogram analysis is a simple, sensitive, and robust way to quantify diffuse pathological changes as it captures the distribution of diffusivity values across the whole brain (Tofts et al., 2003). Studies already showed that histogram measures (such as peak height) can capture disease burden in SVD and correlate with cognition both cross-sectionally (Lawrence et al., 2013) and in longitudinal studies (Holtmannspotter et al., 2005; Molko et al., 2002). However, an unresolved issue was the prominent contamination of whole brain MD data through CSF. Skeletonization overcomes this problem by focusing on the main fiber tracts (Metzler-Baddeley, O'Sullivan, Bells, Pasternak, & Jones, 2012). Nonetheless, residual CSF contamination can be found in certain parts of the skeleton, such as the fornix (Berlot, Metzler-Baddeley, Jones, & O'Sullivan, 2014). We therefore applied a custom mask to remove these areas from the skeleton. This procedure efficiently eliminates the CSF peak in the histogram as a prerequisite to calculating the peak width. As a result, PSMD outperforms traditional MD histogram measures (such as whole brain MD peak height) in terms of the association with processing speed, sample size estimates, and inter-scanner reproducibility.

We found samples with the same diagnosis but recruited through different studies to have remarkably similar PSMDs. This specifically applies to healthy controls from VASCAMY and ADNI, and to population-based elderly subjects from the ASPFS (see Fig 4). The stability of this marker across studies might again relate to the quantitative nature of DTI. Furthermore, it has already been suggested that DTI parameters in general (Grech-Sollars et al., 2015) and MD histogram metrics in particular (Cercignani, Bammer, Sormani, Fazekas, & Filippi, 2003) are largely reproducible across different scanners and sequences. While we cannot fully exclude an influence of scanner type, field strength, and different software versions on MD values (Gunda et al., 2014), our inter-scanner reproducibility study using two scanners with different field strengths showed the best reproducibility for PSMD. It is plausible that PSMD is less prone to inter-scanner and inter-study differences than other

DTI (histogram) parameters, since peak width does not depend on absolute MD values but rather on the distribution pattern of the histogram.

The comparison with healthy controls and patients with AD pathology (ADNI sample) suggests a strong link between our new marker and SVD. PSMD values in MCI patients with a low WMH load and in demented subjects with a low WMH load were not significantly different from healthy controls. However, subgroups with high WMH load showed increases in PSMD. This suggests that also in AD patients, PSMD mostly captures the SVD-related alterations and not primary neurodegenerative pathology. Given the frequent co-occurrence of AD and SVD in the elderly, tools that allow disentangling the vascular contribution to disease burden are of great interest (Prins & Scheltens, 2015). Our results suggest that PSMD may serve that purpose.

An important application of PSMD might be the use as a marker for treatment response in clinical trials. The longitudinal analysis with sample size estimations supports this view, as PSMD had the smallest sample size estimate among all variables. Although the longitudinal analysis was limited to CADASIL subjects, comparing our results with a recent study in sporadic SVD patients suggests good generalizability (Benjamin et al., 2016). In line with our analysis, the previous study demonstrated that WMH volume and whole brain MD peak height were able to reduce the required sample size in clinical trials. Our results extend these findings by demonstrating that PSMD can reduce the sample size even further. Moreover, the excellent inter-scanner reproducibility suggests that PSMD might be particularly suited for multicenter trials.

A major strength of this study is the validation approach involving multiple large samples. These samples were recruited through different settings and covered a broad spectrum of SVD severity. Each study had a prospective design with standardized MRI and comprehensive clinical examination. Also, major conventional MRI markers were obtained for all samples with SVD. This enabled us to determine the relative importance of our new marker in four independent studies. Another strength is the focus on a robust and easy-to-implement marker, which should greatly facilitate the implementation in future studies. The processing pipeline is provided online at www.psmd-marker.com. Given the simple processing steps involved, it is possible to perform the calculation on scanner software directly after image reconstruction within minutes and without any manual intervention.

Our study also has limitations. The use of data from different studies resulted in some differences in scanner field strength, DTI b-values (ranging from 900 to 1200 s/mm^2), and neuropsychological tests utilized to assess processing speed. In addition, there were slight differences in the protocols used for calculating conventional imaging markers and for pre-processing of DTI data. These differences limit comparisons between samples. However, they can also be regarded as a strength. In fact, our findings illustrate the robustness of PSMD under different settings. RUN DMC patients were on average relatively young and mildly affected, which might limit the generalizability of our findings towards older cohorts at later stages of the disease. However, patients with later disease stages were included in the memory clinic sample. A potential limitation for the future application of PSMD is that the co-occurrence of large, non-SVD lesions (e.g. territorial infarcts or tumors) might impede the automatic calculation of PSMD, as they would have to be manually excluded from the analysis. However, such pathologies are rare in SVD patients and accordingly, they were absent in all our samples. Another limitation is the mainly cross-sectional design. To strengthen our results, we chose advanced statistical methods, such as model decomposition, and included multiple validation samples. Nevertheless, the sensitivity of PSMD in capturing disease progression can only be determined by longitudinal studies. More detailed follow-up studies are needed to determine the value of PSMD as a prognostic marker and to further explore its use as a surrogate marker in clinical trials.

In conclusion, this study presents a novel imaging marker, which we consider to be a major step forward in SVD research. We expect the marker to be of great utility for research studies and potentially also for clinical use.

Acknowledgments

This study has been funded by the LMU FöFoLe program (Reg.Nr. 808), the Else Kröner-Fresenius-Stiftung (2014_A200), and the Vascular Dementia Research Foundation. Dr. Ewers received funding from the European Commission (PCIG12-GA-2012-334259). Dr. de Leeuw is supported by the Netherlands Organisation for Scientific Research (grant number 016.126.351). The research of Dr. Biessels and the Utrecht VCI Study group is supported by grant 2010T073 from the Dutch Heart Association and Vidi grant 91711384 from ZonMw, The Netherlands Organisation for Health Research and Development. Dr. Dichgans is

supported by ERA-NET NEURON within the sixth European Union Framework Programme (FP6) (grant 01 EW1207). Part of this project was funded by the the Alzheimer's Disease Neuroimaging Initiative (ADNI) (National Institutes of Health Grant U01 AG024904) and DOD ADNI (Department of Defense award number W81XWH-12-2-0012). ADNI is funded by the National Institute on Aging and the National Institute of Biomedical Imaging and Bioengineering. Private sector contributions are facilitated by the Foundation for the National Institutes of Health (www.fnih.org). A list of industry contributions can be found here: http://adni.loni.usc.edu/about/funding/.

Author Contributions

E.B. collected, analyzed, and interpreted data, and drafted the manuscript and figures. B.G., R.A., A.M.T., M.B., H.L.K., S.R. and E.J. collected and analyzed data, and provided critical revision on the manuscript. H.C., B.E.-W., M.E., R.S., F.-E.L., G.J.B., M.Di. interpreted data and provided critical revision on the manuscript. M.Du. designed and supervised the study, interpreted data, and contributed to the drafting of the manuscript.

Potential Conflicts of Interest

Nothing to report.

2.1.6. References

Aalten, P., Ramakers, I. H. G. B., Biessels, G. J., de Deyn, P. P., Koek, H. L., OldeRikkert, M. G. M., … van der Flier, W. M. (2014). The Dutch Parelsnoer Institute--Neurodegenerative diseases; methods, design and baseline results. *BMC Neurology*, *14*, 254. https://doi.org/10.1186/s12883-014-0254-4

Benjamin, P., Zeestraten, E., Lambert, C., Chis Ster, I., Williams, O. A., Lawrence, A. J., … Markus, H. S. (2016). Progression of MRI markers in cerebral small vessel disease: Sample size considerations for clinical trials. *Journal of Cerebral Blood Flow & Metabolism*, *36*(1), 228–240. https://doi.org/10.1038/jcbfm.2015.113

Berlot, R., Metzler-Baddeley, C., Jones, D. K., & O'Sullivan, M. J. (2014). CSF contamination contributes to apparent microstructural alterations in mild cognitive impairment. *NeuroImage*, *92*, 27–35. https://doi.org/10.1016/j.neuroimage.2014.01.031

Cercignani, M., Bammer, R., Sormani, M. P., Fazekas, F., & Filippi, M. (2003). Inter-sequence and inter-imaging unit variability of diffusion tensor MR imaging histogram-derived metrics of the brain in healthy volunteers. *American Journal of Neuroradiology*, *24*(4), 638–643.

Charidimou, A., & Werring, D. J. (2012). Cerebral microbleeds and cognition in cerebrovascular disease: An update. *Journal of the Neurological Sciences*, *322*(1–2), 50–55. https://doi.org/10.1016/j.jns.2012.05.052

De Groot, M., Verhaaren, B. F. J., de Boer, R., Klein, S., Hofman, A., van der Lugt, A., … Vernooij, M. W. (2013). Changes in Normal-Appearing White Matter Precede Development of White Matter Lesions. *Stroke*, *44*(4), 1037–1042. https://doi.org/10.1161/STROKEAHA.112.680223

De Guio, F., Reyes, S., Duering, M., Pirpamer, L., Chabriat, H., & Jouvent, E. (2014). Decreased T1 contrast between gray matter and normal-appearing white matter in CADASIL. *American Journal of Neuroradiology*, *35*(1), 72–6. https://doi.org/10.3174/ajnr.A3639

Decarli, C., Maillard, P., & Fletcher, E. (2013). Four Tissue Segmentation in ADNI II.

Duering, M., Csanadi, E., Gesierich, B., Jouvent, E., Herve, D., Seiler, S., … Dichgans, M. (2013). Incident lacunes preferentially localize to the edge of white matter

hyperintensities: insights into the pathophysiology of cerebral small vessel disease. *Brain*, *136*(9), 2717–2726. https://doi.org/10.1093/brain/awt184

Duering, M., Zieren, N., Hervé, D., Jouvent, E., Reyes, S., Peters, N., … Dichgans, M. (2011). Strategic role of frontal white matter tracts in vascular cognitive impairment: a voxel-based lesion-symptom mapping study in CADASIL. *Brain*, *134*(8), 2366–2375. https://doi.org/10.1093/brain/awr169

Faul, F., Erdfelder, E., Lang, A.-G., & Buchner, A. (2007). G*Power 3: a flexible statistical power analysis program for the social, behavioral, and biomedical sciences. *Behavior Research Methods*, *39*(2), 175–91. https://doi.org/10.3758/BF03193146

Fox, J., & Weisberg, S. (2011). *An R companion to applied regression.* Sage Publications.

Frisoni, G. B., Fox, N. C., Jack, C. R., Scheltens, P., & Thompson, P. M. (2010). The clinical use of structural MRI in Alzheimer disease. *Nature Reviews. Neurology*, *6*(2), 67–77. https://doi.org/10.1038/nrneurol.2009.215

Ghadery, C., Pirpamer, L., Hofer, E., Langkammer, C., Petrovic, K., Loitfelder, M., … Schmidt, R. (2015). R2* mapping for brain iron: Associations with cognition in normal aging. *Neurobiology of Aging*, *36*(2), 925–932. https://doi.org/10.1016/j.neurobiolaging.2014.09.013

Grech-Sollars, M., Hales, P. W., Miyazaki, K., Raschke, F., Rodriguez, D., Wilson, M., … Clark, C. A. (2015). Multi-centre reproducibility of diffusion MRI parameters for clinical sequences in the brain. *NMR in Biomedicine*, *28*(4), 468–485. https://doi.org/10.1002/nbm.3269

Grömping, U. (2006). R package relaimpo: relative importance for linear regression. *Journal Of Statistical Software*, *17*(1), 139–147. https://doi.org/10.1016/j.foreco.2006.08.245

Gunda, B., Porcher, R., Duering, M., Guichard, J. P., Mawet, J., Jouvent, E., … Chabriat, H. (2014). ADC histograms from routine DWI for longitudinal studies in cerebral small vessel disease: A field study in CADASIL. *Plos One*, *9*(5). https://doi.org/10.1371/journal.pone.0097173

Holtmannspötter, M., Peters, N., Opherk, C., Martin, D., Herzog, J., Bruckmann, H., … Dichgans, M. (2005). Diffusion magnetic resonance histograms as a surrogate marker and predictor of disease progression in CADASIL: a two-year follow-up study. *Stroke*, *36*(12), 2559–2565. https://doi.org/10.1161/01.STR.0000189696.70989.a4

Jokinen, H., Schmidt, R., Ropele, S., Fazekas, F., Gouw, A. A., Barkhof, F., … Erkinjuntti, T. (2013). Diffusion changes predict cognitive and functional outcome: The LADIS study. *Annals of Neurology*, *73*(5), 576–583. https://doi.org/10.1002/ana.23802

Lawrence, A. J., Patel, B., Morris, R. G., MacKinnon, A. D., Rich, P. M., Barrick, T. R., & Markus, H. S. (2013). Mechanisms of cognitive impairment in cerebral small vessel disease: Multimodal MRI results from the St George's Cognition and Neuroimaging in Stroke (SCANS) Study. *Plos One*, *8*(4). https://doi.org/10.1371/journal.pone.0061014

Maillard, P., Fletcher, E., Harvey, D., Carmichael, O., Reed, B., Mungas, D., & DeCarli, C. (2011). White Matter Hyperintensity Penumbra. *Stroke*, *42*(7), 1917–1922. https://doi.org/10.1161/STROKEAHA.110.609768

Metzler-Baddeley, C., O'Sullivan, M. J., Bells, S., Pasternak, O., & Jones, D. K. (2012). How and how not to correct for CSF-contamination in diffusion MRI. *Neuroimage*, *59*(2), 1394–1403. https://doi.org/10.1016/j.neuroimage.2011.08.043

Molko, N., Pappata, S., Mangin, J. F., Poupon, F., LeBihan, D., Bousser, M. G., & Chabriat, H. (2002). Monitoring Disease Progression in CADASIL With Diffusion Magnetic Resonance Imaging: A Study With Whole Brain Histogram Analysis. *Stroke*, *33*(12), 2902–2908. https://doi.org/10.1161/01.STR.0000041681.25514.22

Nitkunan, A., Barrick, T. R., Charlton, R. a., Clark, C. a., & Markus, H. S. (2008). Multimodal MRI in cerebral small vessel disease: Its relationship with cognition and sensitivity to change over time. *Stroke*, *39*(7), 1999–2005. https://doi.org/10.1161/STROKEAHA.107.507475

Nucifora, P. G. P., Verma, R., Lee, S.-K., & Melhem, E. R. (2007). Diffusion-tensor MR imaging and tractography: exploring brain microstructure and connectivity. *Radiology*, *245*(2), 367–384. https://doi.org/10.1148/radiol.2452060445

O'Sullivan, M., Jouvent, E., Saemann, P. G., Mangin, J.-F., Viswanathan, A., Gschwendtner, A., … Dichgans, M. (2008). Measurement of brain atrophy in subcortical vascular disease: A comparison of different approaches and the impact of ischaemic lesions. *NeuroImage*, *43*(2), 312–320. https://doi.org/10.1016/j.neuroimage.2008.07.049

Otsu, N. (1979). A threshold selection method from gray-level histograms. *IEEE Transactions on Systems, Man, and Cybernetics*, *9*(1), 62–66. https://doi.org/10.1109/TSMC.1979.4310076

Pantoni, L. (2010). Cerebral small vessel disease: from pathogenesis and clinical characteristics to therapeutic challenges. *The Lancet. Neurology*, *9*(7), 689–701. https://doi.org/10.1016/S1474-4422(10)70104-6

Patel, B., & Markus, H. S. (2011). Magnetic Resonance Imaging in Cerebral Small Vessel Disease and its Use as a Surrogate Disease Marker. *International Journal of Stroke*, *6*(1), 47–59. https://doi.org/10.1111/j.1747-4949.2010.00552.x

Petersen, R. C. (2004). Mild cognitive impairment as a diagnostic entity. *Journal of internal medicine, 256*(3), 183-194. https://doi.org/10.1111/j.1365-2796.2004.01388.x

Prins, N. D., & Scheltens, P. (2015). White matter hyperintensities, cognitive impairment and dementia: an update. *Nature Reviews. Neurology*, *11*(3), 157–165. https://doi.org/10.1038/nrneurol.2015.10

R core team (2014). *R: A Language and Environment for Statistical Computing.* R Foundation for Statistical Computing, Vienna, Austria. URL https://www.r-project.org/

Smith, E. E., Schneider, J. A., Wardlaw, J. M., & Greenberg, S. M. (2012). Cerebral microinfarcts: the invisible lesions. *The Lancet Neurology, 11*(3), 272-282. https://doi.org/10.1016/S1474-4422(11)70307-6

Smith, S. M., Jenkinson, M., & Johansen-Berg, H. (2006). Tract-based spatial statistics: voxelwise analysis of multi-subject diffusion data. *Neuroimage*, *31*(4), 1487–1505. https://doi.org/10.1016/j.neuroimage.2006.02.024

Smith, S. M., Jenkinson, M., Woolrich, M. W., Beckmann, C. F., Behrens, T. E., Johansen-Berg, H., ... & Niazy, R. K. (2004). Advances in functional and structural MR image analysis and implementation as FSL. *Neuroimage, 23*, S208-S219. https://doi.org/10.1016/j.neuroimage.2004.07.051

Tofts, P. S., Davies, G. R., & Dehmeshki, J. (2003). Histograms: measuring subtle diffuse disease. In *Quantitative MRI of the Brain* (pp. 581–610). John Wiley & Sons, Ltd. https://doi.org/10.1002/0470869526.ch18

Tombaugh, T. N. (2004). Trail Making Test A and B: Normative data stratified by age and education. *Archives of Clinical Neuropsychology*, *19*(2), 203–214. https://doi.org/10.1016/S0887-6177(03)00039-8

Tuladhar, A. M., van Norden, A. G. W., de Laat, K. F., Zwiers, M. P., van Dijk, E. J., Norris, D. G., & de Leeuw, F.-E. (2015). White matter integrity in small vessel disease is related to cognition. *Neuroimage: Clinical*, *7*, 518–524. https://doi.org/10.1016/j.nicl.2015.02.003

Van Der Elst, W., van Boxtel, M. P., van Breukelen, G. J., & Jolles, J. (2007). Assessment of information processing in working memory in applied settings: the paper & pencil memory scanning test. *Psychological medicine,* 37(9), 1335-1344. https://doi.org/10.1017/S0033291707000360

Van der Elst, W., van Boxtel, M. P. J., van Breukelen, G. J. P., & Jolles, J. (2006). The Letter Digit Substitution Test: normative data for 1,858 healthy participants aged 24–81 from the Maastricht Aging Study (MAAS): Influence of Age, Education, and Sex. *Journal of Clinical and Experimental Neuropsychology*, *28*(6), 998–1009. https://doi.org/10.1080/13803390591004428

Van Norden, A. G., de Laat, K. F., Gons, R. A., van Uden, I. W., van Dijk, E. J., van Oudheusden, L. J., ... & Tendolkar, I. (2011). Causes and consequences of cerebral small vessel disease. The RUN DMC study: a prospective cohort study. Study rationale and protocol. *BMC Neurology, 11*(1), 29. https://doi.org/10.1186/1471-2377-11-29

Van Norden, A. G. W., de Laat, K. F., van Dijk, E. J., van Uden, I. W. M., van Oudheusden, L. J. B., Gons, R. A. R., … de Leeuw, F.-E. (2012a). Diffusion tensor imaging and cognition in cerebral small vessel disease. *Biochimica et Biophysica Acta (BBA) - Molecular Basis of Disease*, *1822*(3), 401–407. https://doi.org/10.1016/j.bbadis.2011.04.008

Van Norden, A. G. W., van Uden, I. W. M., de Laat, K. F., van Dijk, E. J., & de Leeuw, F.-E. (2012b). Cognitive function in small vessel disease: the additional value of diffusion tensor imaging to conventional magnetic resonance imaging: the RUN DMC study. *Journal of Alzheimer's Disease*, *32*(3), 667–76. https://doi.org/10.3233/JAD-2012-120784

Viswanathan, A., Godin, O., Jouvent, E., O'Sullivan, M., Gschwendtner, A., Peters, N., … Chabriat, H. (2010). Impact of MRI markers in subcortical vascular dementia: A multi-modal analysis in CADASIL. *Neurobiology of Aging*, *31*(9), 1629–1636. https://doi.org/10.1016/j.neurobiolaging.2008.09.001

Wardlaw, J. M., Smith, E. E., Biessels, G. J., Cordonnier, C., Fazekas, F., Frayne, R., … Dichgans, M. (2013). Neuroimaging standards for research into small vessel disease and its contribution to ageing and neurodegeneration. *The Lancet Neurology*, *12*(8), 822–838. https://doi.org/10.1016/S1474-4422(13)70124-8

Wardlaw, J. M., Hernάndez, M. C. V., & Muñoz‐Maniega, S. (2015). What are white matter hyperintensities made of? Relevance to vascular cognitive impairment. *Journal of the American Heart Association, 4*(6), e001140. https://doi.org/10.1161/JAHA.114.001140

Zwiers, M. P. (2010). Patching cardiac and head motion artefacts in diffusion-weighted images. *NeuroImage*, *53*(2), 565–575. https://doi.org/10.1016/j.neuroimage.2010.06.014

2.1.7. Supplementary Materials

Table e-1. MRI acquisition parameters

Sequence		CADASIL Exploratory	CADASIL Validation	CADASIL Rescan 1.5T	RUN DMC	Utrecht	ADNI	ASPS
T1	TR [ms]	22	2500	-	2250	7.9	400	-
	TE [ms]	6	4.37	-	3.68	4.5	Min full	-
	Slice [mm]	1.2	1	-	1	1	1.2	-
	In-plane [mm]	0.90x0.90	1x1	-	1x1	1x1	1.02x1.02	-
T2	TR [ms]	3300	6500	-	800	3198	-	-
	TE [ms]	95	117	-	26	140	-	-
	Slice [mm]	5	3.3	-	6	3	-	-
	In-plane [mm]	0.94x0.94	1x1	-	1.3x1.0	0.96x0.96	-	-
FLAIR	TR [ms]	8402	5000	-	9000	11000	11000	-
	TE [ms]	151	395	-	84	125	147	-
	TI [ms]	2002	1800	-	2200	2800	2250	-
	Slice [mm]	5	1	-	5	3	5	-
	In-plane [mm]	0.94x0.94	1x1	-	1x1.2	0.96x0.96	0.86x0.86	-
T2*	TR [ms]	1040	742	-	800	1653	-	-
	TE [ms]	22	19.9	-	26	20	-	-
	Slice [mm]	5	5	-	6	3	-	-
	In-plane [mm]	0.94x0.94	1x1	-	1.3x1.0	0.96x0.96	-	-
DTI	TR [ms]	8300	12700	10700	10100	6638	13000	6700
	TE [ms]	96	81	105	93	73	68	95
	Slice [mm]	5	2	2	2.5	2.5	2.7	2.5
	In-plane [mm]	0.94x0.94	2x2	2x2	2.5x2.5	1.72x1.72	1.37x1.37	1.95x1.95
	b-value [s/mm^2]	1000	1000	1000	900	1200	1000	1000
	Directions	41	30	30	30	45	41	4 x 12

DTI=diffusion tensor imaging; FLAIR=fluid attenuation inversion recovery; TE=echo time; TI=inversion time; TR=repetition time.

Table e-2. Linear regression models with processing speed score as dependent variable

	B	SE	Beta	p-value	adj. R^2
CADASIL exploratory sample (n=104): Simple linear regression					
PSMD	-2633.432	279.684	-0.682	1.6×10^{-15}	0.460
Whole brain MD peak height	1915.902	227.733	0.640	2.6×10^{-13}	0.404
BPF	6.784	1.261	0.474	4.9×10^{-7}	0.217
Normalized lacune volume	-770.396	172.786	-0.411	2.2×10^{-5}	0.160
Age	-0.031	0.007	-0.392	3.9×10^{-5}	0.145
Microbleed count	-0.046	0.011	-0.384	7.3×10^{-5}	0.139
Normalized WMH volume	-4.044	1.066	-0.356	2.6×10^{-4}	0.118
Sex	0.082	0.150	0.054	0.586	-0.007
CADASIL exploratory sample: Stepwise model ($p=2.2 \times 10^{-16}$, $R^2=0.539$)					
PSMD	-3415.951	402.965	-0.886	2.8×10^{-13}	-
Normalized WMH volume	4.256	1.167	0.375	4.3×10^{-4}	-
Normalized lacune volume	-367.875	140.077	-0.196	0.010	-
CADASIL validation sample (VASCAMY) (n=57): Simple linear regression					
PSMD	-2356.661	422.689	-0.601	7.7×10^{-7}	0.350
Microbleed count	-0.019	0.005	-0.451	4.4×10^{-4}	0.189
Normalized lacune volume	-448.614	170.501	-0.334	0.011	0.096
Age	-0.017	0.009	-0.262	0.049	0.052
BPF	3.260	2.005	0.214	0.110	0.029
Normalized WMH volume	-2.490	1.560	-0.211	0.116	0.027
Sex	-0.021	0.198	-0.014	0.916	-0.018
CADASIL validation sample: Stepwise model ($p=1.9 \times 10^{-6}$, $R^2=0.363$)					
PSMD	-2157.414	439.283	-0.550	8.7×10^{-6}	-
Normalized lacune volume	-222.581	150.284	-0.165	0.144	-
Sporadic SVD (RUN DMC) (n=436): Simple linear regression					
PSMD	-6428.421	983.184	-0.299	1.8×10^{-10}	0.088
Normalized WMH volume	-22.266	4.881	-0.214	6.6×10^{-6}	0.044
Normalized lacune volume	-2408.848	583.571	-0.194	4.4×10^{-5}	0.036
BPF	5.932	1.481	0.189	7.3×10^{-5}	0.033
Microbleed count	-0.093	0.029	-0.153	0.001	0.021
Age	-0.028	0.009	-0.153	0.001	0.021
Sex	0.354	0.155	0.109	0.023	0.010
Sporadic SVD (RUN DMC): Stepwise model ($p=1.8 \times 10^{-10}$, $R^2=0.088$)					
PSMD	-6428.421	983.184	-0.299	1.8×10^{-10}	-
Memory clinic SVD (high WMH) (Utrecht) (n=47): Simple linear regression					
PSMD	-2893.085	915.687	-0.426	0.003	0.163
Age	0.033	0.011	0.413	0.004	0.152
Normalized WMH volume	-7.838	3.987	-0.281	0.056	0.059
Sex	-0.181	0.152	-0.175	0.240	0.009
Microbleed count	0.035	0.033	0.157	0.293	0.003
BPF	-0.869	2.646	-0.049	0.744	-0.020
Normalized lacune volume	-135.702	549.274	-0.037	0.806	-0.021
Memory clinic SVD (high WMH) (Utrecht): Stepwise model ($p=2.9 \times 10^{-4}$, $R^2=0.278$)					
PSMD	-2553.067	858.943	-0.376	0.005	-
Age	0.029	0.010	0.361	0.007	-

B=Unstandardized coefficient; Beta=Standardized coefficient; BPF=brain parenchymal fraction; MD=mean diffusivity; PSMD=peak width of skeletonized mean diffusivity; SE=standard error of the coefficient; WMH=white matter hyperintensity.

2.2. Study 2: Cortical superficial siderosis in different types of cerebral small vessel disease

Ebru Baykara, MSc[1*], Frank Arne Wollenweber, MD[1*], Marialuisa Zedde, MD[2], Benno Gesierich, PhD[1],Melanie Achmüller[1], Eric Jouvent, MD, PhD[3], Anand Viswanathan, MD, PhD[4], Stefan Ropele, PhD[5], Hugues Chabriat, MD, PhD[3], Reinhold Schmidt, MD[5], Christian Opherk, MD[6], Martin Dichgans, MD[1], Jennifer Linn, MD[7], Marco Duering, MD[1]

[1] Institute for Stroke and Dementia Research, Klinikum der Universität München, Ludwig-Maximilians-Universität LMU, Munich, Germany
[2] Neurology Unit, Stroke Unit, IRCCS-Arcispedale Santa Maria Nuova, Reggio Emilia, Italy
[3] University Paris Diderot, Sorbonne Paris Cité, UMRS 1161 INSERM, Paris, France
[4] Hemorrhagic Stroke Research Program, Department of Neurology, Massachusetts General Hospital Stroke Research Center, Harvard Medical School, Boston, USA
[5] Department of Neurology, Medical University of Graz, Graz, Austria
[6] Klinik für Neurologie, SLK-Kliniken Heilbronn GmbH, Heilbronn, Germany
[7] Institut und Poliklinik für Neuroradiologie, Universitätsklinikum Carl Gustav Carus, Dresden, Germany

*contributed equally

Keywords: Cerebral small vessel disease, Cerebral amyloid angiopathy, CADASIL, magnetic resonance imaging, intracranial hemorrhage

Wollenweber, F. A.*, **Baykara, E**.*, Zedde, M., Gesierich, B., Achmüller, M., Jouvent, E., Viswanathan, A., Ropele, S., Chabriat, H., Schmidt, R., Opherk, C., Dichgans, M., Linn, J. & Duering, M. (2017). Cortical superficial siderosis in different types of cerebral small vessel disease. *Stroke, 48(5),* 1404-1407.

2.2.1. Abstract

Background and Purpose: Cortical superficial siderosis (cSS) has emerged as a clinically relevant imaging feature of cerebral amyloid angiopathy (CAA). However, it remains unknown if cSS is also present in non-amyloid associated small vessel disease (SVD), and if patients with cSS differ in terms of other SVD imaging features.

Methods: 364 CADASIL patients, 372 population-based controls (PC) and 100 CAA patients with cSS (fulfilling the modified Boston criteria for possible/probable CAA) were included. cSS and cerebral microbleeds (CMB) were visually rated on T2*-weighted MRI. White matter hyperintensities (WMH) were segmented on FLAIR images and their spatial distribution was compared between groups using colocalization analysis. CMB location was determined in an observer-independent way using an atlas in standard space.

Results: cSS was absent in CADASIL and present in only 2 (0.5%) PC. CMB were present in 64% of CAA patients with cSS, 34% of CADASIL patients and 12% of PC. Among patients with CMB, lobar location was found in 95% of CAA patients with cSS, 48% of CADASIL patients and 69% of PC. The spatial distribution of WMH was comparable between CAA with cSS and CADASIL as indicated by high colocalization coefficients.

Conclusions: cSS was absent in CADASIL while other SVD imaging features were similar to CAA patients with cSS. Our findings suggest that cSS in combination with other SVD imaging markers is highly indicative of CAA.

2.2.2. Introduction

Cortical superficial siderosis (cSS) has recently been recognized as an imaging marker with high prognostic relevance in patients with cerebral amyloid angiopathy (CAA) (Charidimou et al., 2015). The presence of cSS is associated with intracranial hemorrhage (Linn et al., 2013; Roongpiboonsopit et al., 2016), transient focal neurological episodes and cognitive decline (Wollenweber et al., 2014). However, little is known about the specificity of this marker. In particular, it remains unknown if non-amyloid associated small vessel disease (SVD) may also present with cSS.

Patients with CADASIL (cerebral autosomal dominant arteriopathy with subcortical infarcts and leukoencephalopathy) develop SVD at young age. Hence, this hereditary disease serves as a model for pure and severe non-amyloid associated SVD.

The objectives of the current study are i) to determine whether cSS is also present in SVD types other than CAA, and ii) to compare the patterns of SVD tissue lesions in CAA with cSS to those observed in other types of SVD. Therefore, we first determine the prevalence of cSS in CADASIL patients and a population-based sample. Second, we systematically compare SVD imaging features, i.e. cerebral microbleeds (CMB) and white matter hyperintensities (WMH) between CAA with cSS, CADASIL and population-based controls (PC).

2.2.3. Methods

Detailed methods are provided in the online-only data supplement.

Subjects

Subjects were drawn from 3 prospective studies: 364 CADASIL patients from the Paris-Munich study (Duering et al., 2013), 372 population-based, healthy subjects from the Austrian Stroke Prevention Family Study (ASPFS) (Ghadery et al., 2015) and 100 subjects with cSS and possible/probable CAA from the SuSPect-CAA study (NCT01856699).

MRI

CMB (Wardlaw et al., 2013) and cSS were identified on T2*-weighted gradient echo images by two trained raters (FAW and EB). WMH of presumed vascular origin (Wardlaw et al., 2013) were segmented on FLAIR images. Segmented lesion masks were registered to a common standard space.

Statistical analysis

Analyses were performed in R (v3.2.2). Differences in characteristics and SVD lesion load between samples were analyzed using the Kruskal-Wallis test with Dunn post-hoc tests (for continuous variables, R package 'PMCMR') or chi-square tests with post-hoc tests (for categorical variables, R package 'fifer'). To account for multiple comparisons, all p-values were Bonferroni-corrected. The similarity of the WMH distribution between samples was evaluated by a colocalization analysis using linear correlation on voxel-wise lesion frequencies.

2.2.4. Results

Demographic, clinical and MRI characteristics of the study samples and the results of group comparisons are presented in Table 1.

While CADASIL patients showed severe SVD imaging features (Table 1, Figure 1A), cSS was absent in the entire sample. Only 2 subjects from the population-based sample had cSS. One of them also had a high number of lobar CMB (n=28), suggesting the presence of CAA.

We next compared the spatial distribution of CMB and WMH between samples (Figure 1B, Figure 2). CMB in CADASIL were predominantly deep and infratentorial. However, among CADASIL patients with CMB, lobar areas were affected in nearly every second patient and even strictly lobar involvement occurred in one out of ten (Table 1). For WMH, the colocalization analysis showed that lesion distribution was most similar between CAA with cSS and CADASIL (R^2=0.68, $P<10^{-15}$), while colocalization was less strong between CAA with cSS and PC (R^2=0.52, $P<10^{-15}$) as well as CADASIL and PC (R^2=0.31, $P<10^{-15}$).

2.2.5. Discussion

Cortical superficial siderosis is a frequent finding in patients with histologically proven CAA (Linn et al., 2010). The current study demonstrates that cSS is absent in a large cohort of patients with a severe non-amyloid associated SVD due to CADASIL and exceedingly rare in a population-based sample. Hence, our results indicate that cSS is not a general marker for SVD, but strongly indicative of the presence of CAA. This is in line with a recent study, which found positive amyloid PET in 12 cSS cases (Na et al., 2015).

Table 1: Characteristics of the study samples

	CADASIL (Paris-Munich) n=364	PC (ASPFS) n=372	CAA + cSS (SuSPect-CAA) n=100	p-value*
Demographic characteristics				
Age, mean (SD) (min, max) [years]	51.0 (11.4) (22.9, 79.4)	65.0 (10.7) (38.0, 86.0)	73.8 (6.9) (57.0, 89.0)	<0.001/a,b,c
Female, n (%)	202 (55.5)	161 (43.3)	38 (38.0)	0.006/a,c
Vascular risk factors				
Current smoker, n (%)	77 (21.2)	51 (13.7)	n/a	n/a
Past smoker, n (%)	116 (31.9)	113 (30.4)	n/a	n/a
Hypertension, n (%)	78 (21.4)	235 (63.2)	68 (68.0)	<0.001/a,c
Hypercholesterolemia, n (%)	145 (39.8)	279 (75.0)	50 (50.0)	<0.001/b,c
Diabetes, n (%)	10 (2.7)	40 (10.8)	10 (10.0)	<0.001/c
Imaging characteristics				
WMH volume, median (IQR) (min, max) [normalized %]	5.95 (6.17) (0, 27.52)	0.28 (0.40) (0.004, 6.06)	1.57 (2.68) (0.007, 12.60)	<0.001/a,b,c
CMB number, median (IQR) (min, max)	0 (1) (0, 88)	0 (0) (0, 40)	2 (6) (0, 92)	<0.001/a,b,c
Presence of CMB, n (%)	124 (34.1)	16 (4.3)	64 (64.0)	<0.001/a,b,c
Lobar CMB, n (%)†	59 (47.6)	11 (68.8)	61 (95.3)	<0.001/a
Deep CMB, n (%)†	97 (78.2)	6 (37.5)	19 (29.7)	<0.001/a,c
Infratentorial CMB, n (%)†	63 (50.8)	4 (25.0)	2 (18.8)	<0.001/a
Strictly lobar CMB, n (%)†	13 (10.5)	8 (50.0)	44 (68.8)	<0.001/a,c

ASPFS: Austrian Stroke Prevention Family Study; CAA: cerebral amyloid angiopathy; CADASIL: cerebral autosomal dominant arteriopathy with subcortical infarcts and leukoencephalopathy; CMB: cerebral microbleeds; cSS: cortical superficial siderosis; IQR: interquartile range; NA: not available; PC: population-based controls; WMH: white matter hyperintensities.

* Bonferroni corrected; post-hoc group comparisons $p < 0.01$, a: CADASIL vs. cSS, b: cSS vs. PC, c: CADASIL vs. PC.

† Percentage out of patients with CMB.

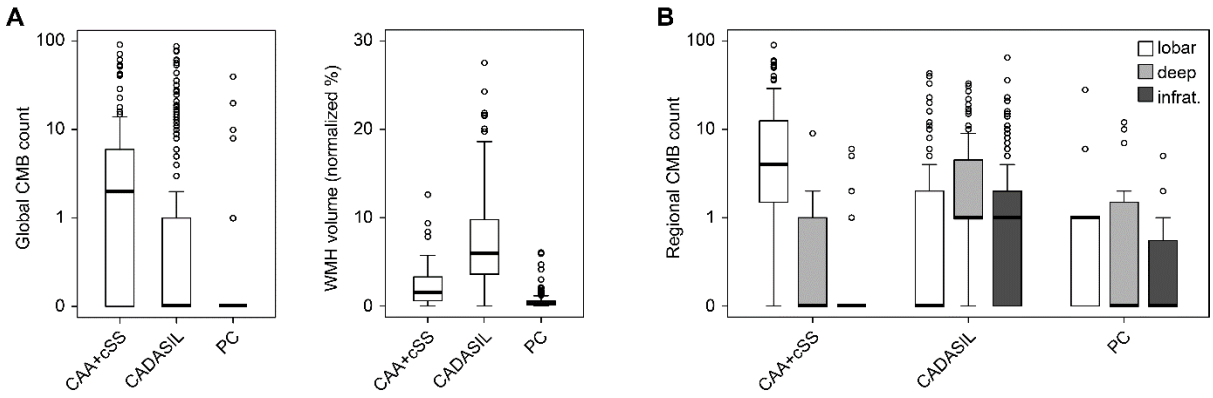

Figure 1. Frequency of CMB and WMH. A. Boxplots for CMB counts and normalized WMH volumes in each sample. **B.** Regional CMB counts (lobar, deep, infratentorial) for patients with at least one CMB. Note the log scale for global and regional CMB count.

Our findings on the frequency and distribution of both CMB and WMH show a substantial overlap between samples and therefore suggest a limited value of these imaging markers in discriminating different forms of SVD. Of note, this also applies to lobar CMB, which are considered typical for CAA.

It is commonly hypothesized that cSS reflects the result of recurrent focal convexity hemorrhages triggered by vascular amyloid (Charidimou et al., 2015). Recent data from Abeta antibody trials in Alzheimer´s disease support this hypothesis: Treatment groups developed cSS in a time, dose and APOE dependent manner (DiFrancesco, Longoni, & Piazza, 2015; Sevigny et al., 2016). Our results suggest that these convexity hemorrhages are typically absent in non-amyloid associated SVD.

Strengths of this study include the prospectively collected data and the large sample sizes in all groups. A potential limitation is the use of different MR field strengths (1.5T and 3T), which might have led to an underestimation of CMB on 1.5T scans. Furthermore, study patients were mostly in early and middle disease stages, precluding definite conclusions for late stages. Still, the samples were well representative for an outpatient clinic setting, in which cSS can be of high utility.

2.2.6. Conclusion

These findings provide further evidence that cSS is an imaging marker for CAA. Longitudinal data are needed to investigate the value of cSS in therapeutic decision-making.

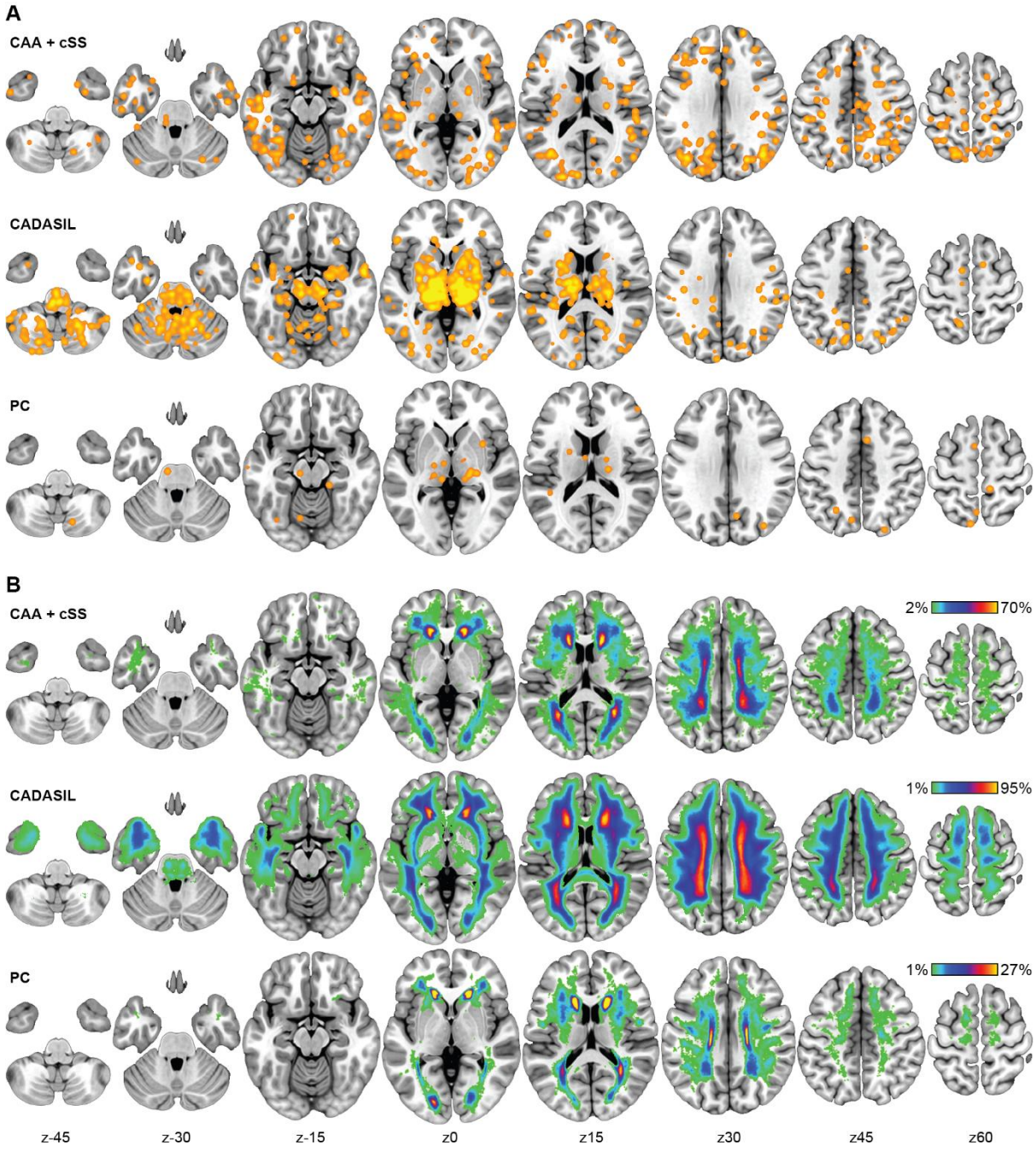

Figure 2. Spatial Distribution of CMB (A) and WMH (B). A. Each sphere represents one CMB in the sample. Maps are superimposed onto the T1 standard space template. **B.** Aside from frequent WMH in the temporal pole in CADASIL patients, the overall pattern was comparable between the three samples.

Sources of funding

This work was supported by the Ludwig-Maximilians-University "Förderung für Forschung und Lehre (FöFoLe)" program (808), the Else Kröner-Fresenius-Stiftung (2014_A200), and the Vascular Dementia Research Foundation.

Disclosures

None

2.2.7. References

Charidimou, A., Linn, J., Vernooij, M. W., Opherk, C., Akoudad, S., Baron, J. C., … Werring, D. J. (2015). Cortical superficial siderosis: Detection and clinical significance in cerebral amyloid angiopathy and related conditions. *Brain*. https://doi.org/10.1093/brain/awv162

DiFrancesco, J. C., Longoni, M., & Piazza, F. (2015). Anti-aβ autoantibodies in amyloid related imaging abnormalities (aria): candidate biomarker for immunotherapy in alzheimer's disease and cerebral amyloid angiopathy. *Frontiers in Neurology*, *6*, 207. https://doi.org/10.3389/fneur.2015.00207

Duering, M., Csanadi, E., Gesierich, B., Jouvent, E., Herve, D., Seiler, S., … Dichgans, M. (2013). Incident lacunes preferentially localize to the edge of white matter hyperintensities: insights into the pathophysiology of cerebral small vessel disease. *Brain*, *136*(9), 2717–2726. https://doi.org/10.1093/brain/awt184

Ghadery, C., Pirpamer, L., Hofer, E., Langkammer, C., Petrovic, K., Loitfelder, M., … Schmidt, R. (2015). R2* mapping for brain iron: Associations with cognition in normal aging. *Neurobiology of Aging*, *36*(2), 925–932. https://doi.org/10.1016/j.neurobiolaging.2014.09.013

Linn, J., Halpin, A., Demaerel, P., Ruhland, J., Giese, A. D., Dichgans, M., … Greenberg, S. M. (2010). Prevalence of superficial siderosis in patients with cerebral amyloid angiopathy. *Neurology*, *74*(17), 1346–1350. https://doi.org/10.1212/WNL.0b013e3181dad605

Linn, J., Wollenweber, F. A., Lummel, N., Bochmann, K., Pfefferkorn, T., Gschwendtner, A., … Opherk, C. (2013). Superficial siderosis is a warning sign for future intracranial hemorrhage. *Journal of Neurology*, *260*(1), 176–181. https://doi.org/10.1007/s00415-012-6610-7

Na, H. K., Park, J. H., Kim, J. H., Kim, H. J., Kim, S. T., Werring, D. J., … Na, D. L. (2015). Cortical superficial siderosis: A marker of vascular amyloid in patients with cognitive impairment. *Neurology*, *84*(8), 849–855. https://doi.org/10.1212/WNL.0000000000001288

Roongpiboonsopit, D., Charidimou, A., William, C. M., Lauer, A., Falcone, G. J., Martinez-Ramirez, S., … Viswanathan, A. (2016). Cortical superficial siderosis predicts early recurrent lobar hemorrhage. *Neurology*, *87*(18), 1863–1870. https://doi.org/10.1212/WNL.0000000000003281

Sevigny, J., Chiao, P., Bussière, T., Weinreb, P. H., Williams, L., Maier, M., … Sandrock, A. (2016). The antibody aducanumab reduces Aβ plaques in Alzheimer's disease. *Nature*, *537*(7618), 50–56. https://doi.org/10.1038/nature19323

Wardlaw, J. M., Smith, E. E., Biessels, G. J., Cordonnier, C., Fazekas, F., Frayne, R., … Dichgans, M. (2013). Neuroimaging standards for research into small vessel disease and its contribution to ageing and neurodegeneration. *The Lancet Neurology*, *12*(8), 822–838. https://doi.org/10.1016/S1474-4422(13)70124-8

Wollenweber, F. A., Buerger, K., Mueller, C., Ertl-Wagner, B., Malik, R., Dichgans, M., … Opherk, C. (2014). Prevalence of cortical superficial siderosis in patients with cognitive impairment. *Journal of Neurology*, *261*(2), 277–282. https://doi.org/10.1007/s00415-013-7181-y

2.2.8. Supplementary materials

Subjects

CADASIL patients were recruited at two centers (Munich and Paris). The diagnosis was confirmed by molecular genetic testing or ultrastructural analysis of a skin biopsy.

The population-based control sample (Austrian Stroke Prevention Family Study, ASPFS) was recruited at a single center (Graz).

Subjects with cortical superficial siderosis (cSS, for examples see Supplemental Figure I) were recruited at two centers (Munich and Reggio Emilia) within the SuSPect-CAA study (NCT01856699). They fulfilled the modified Boston criteria (Linn et al., 2010) for probable (n=79) or possible (n=21) cerebral amyloid angiopathy (CAA). The category 'probable CAA' requires at least one lobar cerebral microbleed (CMB) or hemorrhage in addition to cSS. The category 'possible CAA' requires the presence of cSS in the absence of any other cause than CAA (such as trauma or aneurysm).

All studies were approved by the ethics committees of the respective institutions. Written informed consent was obtained from all subjects.

MRI rating and processing

MRI acquisition parameters are presented in the Supplemental Table I.

Lesions were rated (cSS, CMB) or segmented (white matter hyperintensities, WMH) according to the STRIVE criteria (Wardlaw, Smith, Biessels, et al., 2013). In ambiguous cases regarding cSS, a consensus was reached between the two expert raters (FAW and EB).

WMH segmentation on FLAIR images was performed as previously published for the CADASIL and ASPFS datasets (Duering et al., 2013; Ghadery et al., 2015). For the SuSPect-CAA dataset we used a semi-automated method based on tissue segmentation and clustering-based image thresholding using Otsu's method as previously described (Baykara et al., 2016). Normalized WMH volumes for each sample were calculated by dividing through the volume of the intracranial cavity estimated from T2 (CADASIL, ASPFS) or T2* (SuSPect-CAA) images.

Lesion masks for CMB and WMH were normalized to 1 mm Montreal Neurological Institute (MNI) 152 standard space via 3DT1 images and the registration tools 'FLIRT' and 'FNIRT' from the Functional Magnetic Resonance Imaging of the Brain Software Library (FSL, Smith et al., 2004) (CADASIL and ASPFS). Because 3DT1 images were not available

in the SuSPect-CAA study, we used FLAIR images, a custom-made FLAIR standard space template, and a two-step normalization procedure incorporating the Statistical Parametric Mapping (SPM) 'old normalize' tool (Friston et al., 1995) followed by an additional FNIRT step. All normalization steps were checked visually.

Assessment of the spatial distribution of CMB and WMH

CMB location (lobar, deep, infratentorial) was rated automatically in standard space using a modified version of the MNI structural atlas (Supplemental Figure II) provided within FSL (Mazziotta et al., 2001). This atlas contained lobar region of interests (ROI) as well as the cerebellum. As modification, a brainstem mask was drawn manually and merged with the cerebellar region to create the infratentorial ROI. The deep ROI was defined as brain areas not included in either the lobar or infratentorial ROI.

To compare the distribution of WMH between samples, we performed a colocalization analysis in MNI 152 standard space. For each voxel in standard space, the lesion frequency was entered in a spatial correlation analysis. When correlating the voxel-wise lesion frequencies of two samples, a correlation coefficient of 1 indicates an identical lesion distribution.

Statistical software packages

Analyses were performed in R (v3.2.2; R Core Team, 2014) including the following packages: 'PMCMR' (v4.1; Pohlert, 2014), 'fifer' (v1.0; Fife, 2014), 'ROCR' (v1.0-7; Sing, Sander, Beerenwinkel, & Lengauer, 2005).

2.2.9. Supplementary references

Baykara, E., Gesierich, B., Adam, R., Tuladhar, A. M., Biesbroek, J. M., Koek, H. L., … Duering, M. (2016). A Novel Imaging Marker for Small Vessel Disease Based on Skeletonization of White Matter Tracts and Diffusion Histograms. *Annals of Neurology*, *80*(4), 581–592. https://doi.org/10.1002/ana.24758

Duering, M., Csanadi, E., Gesierich, B., Jouvent, E., Herve, D., Seiler, S., … Dichgans, M. (2013). Incident lacunes preferentially localize to the edge of white matter hyperintensities: insights into the pathophysiology of cerebral small vessel disease. *Brain*, *136*(9), 2717–2726. https://doi.org/10.1093/brain/awt184

Fife, D. (2014). fifer: A collection of miscellaneous functions. R package version, 1.0. URL https://CRAN.R-project.org/package=fifer

Friston, K. J., Ashburner, J., Frith, C. D., Poline, J. B, Heather, J. D., & Frackowiak, R. S. J. (1995). Spatial registration and normalization of images. *Human Brain Mapping*, *3*(3), 165–189. https://doi.org/10.1002/hbm.460030303

Ghadery, C., Pirpamer, L., Hofer, E., Langkammer, C., Petrovic, K., Loitfelder, M., … Schmidt, R. (2015). R2* mapping for brain iron: Associations with cognition in normal aging. *Neurobiology of Aging*, *36*(2), 925–932. https://doi.org/10.1016/j.neurobiolaging.2014.09.013

Linn, J., Halpin, A., Demaerel, P., Ruhland, J., Giese, A. D., Dichgans, M., … Greenberg, S. M. (2010). Prevalence of superficial siderosis in patients with cerebral amyloid angiopathy. *Neurology*, *74*(17), 1346–1350. https://doi.org/10.1212/WNL.0b013e3181dad605

Mazziotta, J., Toga, A., Evans, A., Fox, P., Lancaster, J., Zilles, K., … Mazoyer, B. (2001). A probabilistic atlas and reference system for the human brain: International Consortium for Brain Mapping (ICBM). *Philosophical Transactions of the Royal Society B: Biological Sciences*, *356*(1412), 1293–1322. https://doi.org/10.1098/rstb.2001.0915

Pohlert, T. (2014). The Pairwise Multiple Comparison of Mean Ranks Package (PMCMR). *R Package*, URL https://CRAN.R-project.org/package=PMCMR

R core team (2014). *R: A Language and Environment for Statistical Computing.* R Foundation for Statistical Computing, Vienna, Austria. URL https://www.r-project.org/

Sing, T., Sander, O., Beerenwinkel, N., & Lengauer, T. (2005). ROCR: Visualizing classifier performance in R. *Bioinformatics*, *21*(20), 3940–3941. https://doi.org/10.1093/bioinformatics/bti623

Smith, S. M., Jenkinson, M., Woolrich, M. W., Beckmann, C. F., Behrens, T. E. J., Johansen-Berg, H., … Matthews, P. M. (2004). Advances in functional and structural MR image analysis and implementation as FSL. In *Neuroimage* (Vol. 23). https://doi.org/10.1016/j.neuroimage.2004.07.051

Wardlaw, J. M., Smith, E. E., Biessels, G. J., Cordonnier, C., Fazekas, F., Frayne, R., … Dichgans, M. (2013). Neuroimaging standards for research into small vessel disease and its contribution to ageing and neurodegeneration. *The Lancet Neurology*, *12*(8), 822–838. https://doi.org/10.1016/S1474-4422(13)70124-8

2.2.10. Supplementary tables

Supplementary Table I: MRI parameters

Sequence		**CADASIL (Paris-Munich)**			**ASPFS**	**SuSPect-CAA**	
	Scanner*	**Munich Vision**	**Munich Signa**	**Paris**		**Munich**	**Reggio Emilia**
	Patients [n]	49	71	244	372	36	64
T1	TR [ms]	11.4	22	8.6	1900	-	-
	TE [ms]	4.4	6	1.9	2.19	-	-
	Slice [mm]	1.2	1	0.8	1	-	-
	In-plane [mm]	0.90	0.90	1.02	1	-	-
FLAIR	TR [ms]	4284	8402	8402	10000	8500	11000
	TE [ms]	110	151	161	69	121	140
	TI [ms]	1428	2002	2002	2500	2250	2800
	Slice [mm]	5	5	5.5	3	5.5	5
	In-plane [mm]	0.98	0.94	0.47	0.94	0.43	0.83
T2*	TR [ms]	1056	1040	500	35	600	833
	TE [ms]	22	22	15	19.60	9	23
	Slice [mm]	5	5	5.5	4	5.5	5
	In-plane [mm]	0.94	0.94	0.94	0.90	0.43	0.90

FLAIR: Fluid-attenuated inversion recovery; TE: echo time; TI: inversion time; TR: repetition time.

*Scanner:

CADASIL (Paris-Munich):

Munich Vision: Siemens Magnetom Vision, 1.5 Tesla

Munich Signa: General Electric Signa HD, 1.5 Tesla

Paris: General Electric Signa HD, 1.5 Tesla

SuSPEct-CAA:

Munich: General Electric Signa HDxt, 3.0 Tesla

Reggio Emilia: Philips Achieva, 1.5 Tesla

ASPFS:

Siemens Magnetom Trio, 3.0 Tesla

2.2.11. Supplementary figures

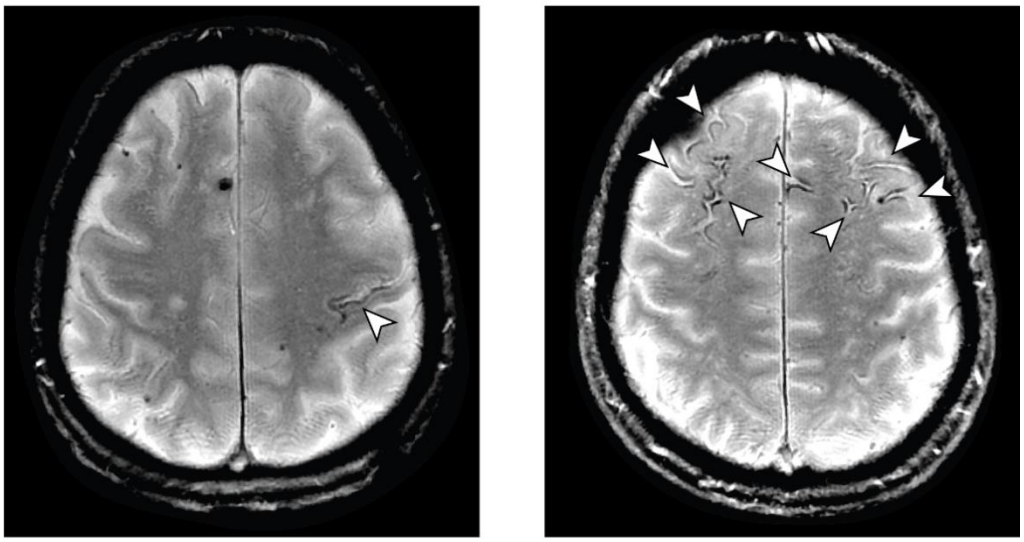

Supplementary Figure I: Cortical superficial siderosis

Two examples for cortical superficial siderosis (cSS, white arrow heads). A case with focal cSS is presented on the left, a case with disseminated cSS (≥ 3 sulci) on the right.

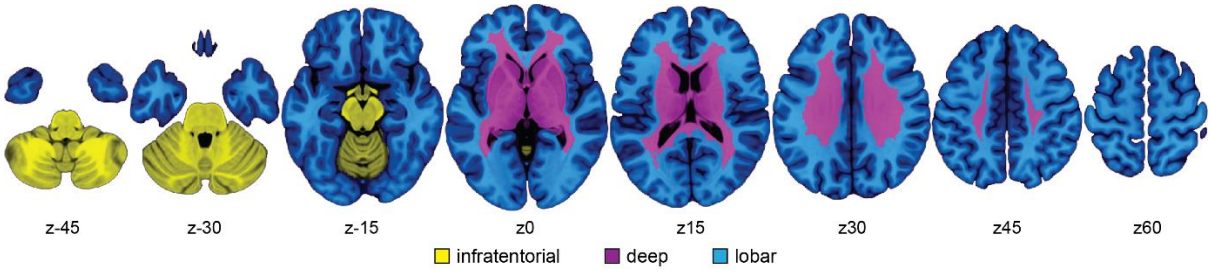

Supplementary Figure II: Atlas for the determination of microbleed location

ROIs are superimposed on the MNI T1 standard space template.

GENERAL DISCUSSION

The work described in this thesis focused on the imaging markers of cerebral small vessel disease. The first project was designed to establish a fully-automated marker of cSVD related microstructural damage, which is strongly associated with the typical cognitive impairment and that could be applied readily to a large number of patients. The second project aimed at investigating and validating the value of cortical superficial siderosis (cSS) as a disease marker for cerebral amyloid angiopathy (CAA), a particular type of cSVD. In this section, the main findings and their implications are discussed, together with suggestions for future directions.

3.1. Imaging markers of cerebral small vessel disease

The small vessels of the brain, which are at the center of the disease, cannot be visualized *in vivo*. Consequently, both subtypes of the disease, arteriolosclerosis and cerebral amyloid angiopathy, rely on brain tissue imaging methods for diagnosis and assessment of disease burden. The first and most important step is diagnosing the patients correctly. This has implication for the information provided to the patients and their caregivers, and the management and treatment of the disease. Furthermore, correct diagnosis is important to understand the underlying pathophysiology. For instance, proper phenotyping by diagnosis is crucial in genetic studies identifying risk genes for a certain disease.

The second step is to have an imaging method/marker, which can quantify the level of tissue damage in the brain reliably. This step is important for evaluating the disease severity, progression and effects of therapeutic interventions. It further helps to expand the knowledge base about the disease, its pathophysiology and the consequences of disease related brain damage.

3.1.1. Diffusion histograms as surrogate markers in cerebral small vessel disease

The project focused on a new surrogate DTI marker for cSVD research, and resulted in the marker PSMD (peak width of skeletonized mean diffusivity), which is now a fully automated, robust and has a high association with the main cognitive deficit of cSVD patients, namely processing speed. The power and utility of PSMD as a marker was independently validated in patients with hereditary and sporadic cSVD as well as in memory clinic patients with a high burden of vascular damage. Furthermore, the study showed that PSMD was primarily linked to vascular pathology, but not to neurodegenerative pathology.

Our results suggest that PSMD is a marker sensitive to cerebrovascular pathology, and can be utilized to assess the cSVD burden in patients.

The main motivation of the project was to avoid the problems associated with conventional disease markers. Conventional markers visible on MRI, such as white matter hyperintensities and lacunes, are manifestations of advanced disease stages (De Groot et al., 2013). At this stage, the brain has already undergone significant changes that enabled these lesions to become visible on standard MRI sequences (T1 and T2 weighted). Furthermore, volumetric measures of these conventional disease markers have only a moderate association with disease related cognitive impairment (Duering et al., 2011; Patel & Markus, 2011). This is likely due to the fact that visible lesions do not always reflect the true burden of the brain damage. Quantitative methods such as DTI have been shown to correlate better with brain damage as well as cognitive deficits (executive function and processing speed) (Holtmannspotter et al., 2005; Nitkunan, Barrick, Charlton, Clark, & Markus, 2008). Importantly, the quantification of the conventional disease markers (lesion volume, or number) relies on manual or semi-automated methods, and almost always requires visual checking and manual editing (Wardlaw et al., 2013). This makes the process highly time-consuming and prone to rater bias and variability. The labour-intensive nature of this process makes the conventional cSVD markers unattractive for large clinical trials. It is plausible that the methodological challenges accompanying the efforts to quantify the disease burden slowed down advances in cSVD research.

Change was introduced with the widespread use of more advanced methods like DTI in the clinical studies. Multiple studies have shown that DTI can measure microstructural damage in the brain more accurately than any of the conventional MRI methods. DTI is sensitive towards detection of brain damage before it becomes visible on conventional MRI (De Groot et al., 2013; Jokinen et al., 2013). Because of this advantage over conventional imaging methods, in the recent years DTI has emerged as the method of choice for investigating cSVD related brain damage.

For cSVD lesions on conventional MRI, multiple studies have shown that the effects of the lesions depend, at least in part, on their location (Duering et al., 2011, 2014). That is why some lesions have more detrimental effects on the clinical outcome than others do. Although there are certain advantages of ROI based approaches in cSVD research, it is fruitful to

analyse the whole brain. First, although the lesion location is an important factor for the effects of lesion burden, cSVD is a diffuse disease, which affects the whole brain. Therefore, researchers could potentially miss important information, if they focus on only certain predefined regions of the brain. Second, it is known that visible lesions are only the tip of the iceberg, and there is hidden damage in so-called "normal appearing" brain tissue as a result of cSVD. Given these points, whole brain approaches are more informative about the overall severity of the disease. Nevertheless, to understand the disease and its specific effects and for particular research questions, it is advisable to follow the global whole brain approach together with an ROI- or voxel-based analysis.

The marker PSMD is a fully automated marker, which demonstrated a stronger association with SVD-related processing speed deficits as compared with all other conventional MRI markers. PSMD also reduced the sample sizes needed in clinical trials markedly. Furthermore, as determined in an inter-scanner reproducibility study, the PSMD marker is stable across different scanners, field strengths and imaging sequences - a characteristic that is desirable for multi-center studies. Therefore, PSMD is particularly suited for clinical routine and for large clinical trials.

3.1.2. Cortical superficial siderosis in cerebral small vessel disease

CSS is a marker, which is often seen in patients with CAA (Linn et al., 2010). The prevalence of cSS is associated with the presence of other imaging markers of cSVD, such as WMH and CMB. It has been shown that CAA and arteriolosclerosis have different preferential distribution of these imaging markers: CMB in CAA are mostly cortical (lobar), but subcortical (deep) in arteriolosclerosis. However, although the presence of lobar microbleeds is included in diagnostic criteria for CAA (Boston criteria and modified Boston criteria), the usefulness of these distribution patterns for differential diagnosis and the specificity of cSS as a marker for CAA were still unknown. Our results demonstrated that the frequency and distribution of WMH and CMB overlap between CAA and arteriolosclerosis, which suggests that these markers have only limited value for discriminating different types of cSVD. More importantly, our findings revealed that cSS was absent in a cohort of severe non-amyloidogenic cSVD patients (CADASIL) and very rare in a population-based sample

comprising patients with sporadic cSVD. Therefore, it can be concluded that the presence of cSS (together with the presence of other SVD markers) is strongly indicative of CAA.

Since CAA can only be diagnosed as definitive after a histological investigation of affected brain tissue, obtained at autopsy or through brain biopsy, the imaging disease manifestations are used as non-invasive diagnosis criteria *in vivo*. The correct diagnosis is crucial, as it may have important implications for decision making regarding disease management, such as using or avoiding certain drugs, in particular anticoagulation.

To date, there are no treatment or preventive strategies available for CAA. The focus is usually on prevention of haemorrhagic events and dementia. CAA patients have an increased risk of intracranial haemorrhage (intracerebral and subarachnoidal), and this risk is further increased for those patients who use antithrombotic drugs (Rosand, Hylek, O'Donnell, & Greenberg, 2000). Elderly patients are usually at risk for both, ischaemic and haemorrhagic cerebrovascular events and it is therefore important to identify CAA patients who have a greatly increased bleeding risk. The vascular changes resulting from CAA pathology together with the use of anticoagulation drugs may lead to the enlargement of small haemorrhages, which would otherwise remain asymptomatic and harmless. In patients with probable CAA, administration of antithrombotic drugs should be avoided as much as possible (Biffi et al., 2010; Charidimou et al., 2017) . Studies also revealed that patients treated with antihypertensive drugs have a reduced risk of CAA-related ICHs (Arima et al., 2010).

3.2. Conclusions

In clinical and in research settings, the first important step when encountering a cSVD patient is to diagnose the patient correctly and differentiate the underlying aetiologies. The main types of cSVD, arteriolosclerosis and cerebral amyloid angiopathy, have different pathogenesis although they share many of the disease manifestations. Differential diagnosis is especially important in decision-making for management and treatment strategies. CAA bears a high risk for spontaneous and anti-coagulative treatment related haemorrhage, and therefore correct diagnosis is the crucial first step for reducing the bleeding risk. We showed that cSS is an important imaging marker for the differential diagnosis of CAA.

In patients with arteriolosclerosis, we proposed a fully-automated method for estimating disease severity. The DTI-based marker 'PSMD' is a major step forward in

accurately determining disease burden in patients' brains and might enable crucial advances in clinical decision-making. We expect that PSMD will play a role in future clinical trials, either for patient selection or as a surrogate marker for treatment effects. The high sensitivity, robustness and accuracy of PSMD might enable identification and study of patients in early disease stages, where preventive strategies could be most effective. As a fully-automated tool, PSMD can be readily implemented in clinical routine and large trials.

3.3. Future steps

Although we included a longitudinal analysis in patients with a genetically-defined cSVD CADASIL, the performance of the marker PSMD is yet to be shown in longitudinal studies of sporadic cSVD patients. Our results of the preliminary longitudinal analyses revealed that PSMD values change over time significantly. PSMD also enables, as a surrogate marker, the smallest sample sizes to be used in comparison to conventional markers - or to clinical scales - in order to reliably detect a treatment effect. Nevertheless, PSMD should be tested in larger longitudinal studies to evaluate its value as a surrogate marker and as a predictor of change over time.

Another future step is to apply PSMD as an imaging marker in CAA patients. Studies have already shown that CAA patients have diffusion changes within their brains (Reijmer et al., 2015; Viswanathan et al., 2008). Since arteriolosclerosis and CAA share many of the disease manifestations, it is plausible that PSMD will be a good marker of disease burden in CAA patients. Considering the preferential distribution of CAA lesions in the lobar brain regions, the calculation of PSMD may be modified.

A DTI sequence should be included in the clinical routine for SVD patients, which could be used to calculate PSMD right after scanning once the fully automated analysis pipeline is implemented in the scanning console. The calculation of PSMD as a reflection of disease burden while also taking into account differential disease markers (e.g. cSS) should give a comprehensive picture about disease aetiology, disease severity and also provide an estimation about the bleeding risk.

While the detection of cSS is currently achieved by visual rating, machine learning algorithms specialized in image analysis (such as convolutional neuronal networks) may provide a way for automated rating in the future.

3.4. References

Arima, H., Tzourio, C., Anderson, C., Woodward, M., Bousser, M. G., MacMahon, S., … Chalmers, J. (2010). Effects of perindopril-based lowering of blood pressure on intracerebral hemorrhage related to amyloid angiopathy: The progress trial. *Stroke*, *41*(2), 394–396. https://doi.org/10.1161/STROKEAHA.109.563932

Biffi, A., Halpin, A., Towfighi, A., Gilson, A., Busl, K., Rost, N., … Viswanathan, A. (2010). Aspirin and recurrent intracerebral hemorrhage in cerebral amyloid angiopathy. *Neurology*, *75*(8), 693–698. https://doi.org/10.1212/WNL.0b013e3181eee40f

Charidimou, A., Boulouis, G., Gurol, M. E., Ayata, C., Bacskai, B. J., Frosch, M. P., … Greenberg, S. M. (2017). Emerging concepts in sporadic cerebral amyloid angiopathy. *Brain*, *140*, (7), 1829–1850. https://doi.org/10.1093/brain/awx047

De Groot, M., Verhaaren, B. F. J., de Boer, R., Klein, S., Hofman, A., van der Lugt, A., … Vernooij, M. W. (2013). Changes in normal-appearing white matter precede development of white matter lesions. *Stroke*, *44*(4), 1037–1042. https://doi.org/10.1161/STROKEAHA.112.680223

Duering, M., Gesierich, B., Seiler, S., Pirpamer, L., Gonik, M., Hofer, E., … Dichgans, M. (2014). Strategic white matter tracts for processing speed deficits in age-related small vessel disease. *Neurology*, *82*(22), 1946–1950. https://doi.org/10.1212/WNL.0000000000000475

Duering, M., Zieren, N., Hervé, D., Jouvent, E., Reyes, S., Peters, N., … Dichgans, M. (2011). Strategic role of frontal white matter tracts in vascular cognitive impairment: a voxel-based lesion-symptom mapping study in CADASIL. *Brain*, *134*(8), 2366–2375. https://doi.org/10.1093/brain/awr169

Holtmannspötter, M., Peters, N., Opherk, C., Martin, D., Herzog, J., Bruckmann, H., … Dichgans, M. (2005). Diffusion magnetic resonance histograms as a surrogate marker and predictor of disease progression in CADASIL: a two-year follow-up study. *Stroke*, *36*(12), 2559–2565. https://doi.org/10.1161/01.STR.0000189696.70989.a4

Jokinen, H., Schmidt, R., Ropele, S., Fazekas, F., Gouw, A. A., Barkhof, F., … Erkinjuntti, T. (2013). Diffusion changes predict cognitive and functional outcome: The LADIS study. *Annals of Neurology*, *73*(5), 576–583. https://doi.org/10.1002/ana.23802

Linn, J., Halpin, A., Demaerel, P., Ruhland, J., Giese, A. D., Dichgans, M., … Greenberg, S. M. (2010). Prevalence of superficial siderosis in patients with cerebral amyloid angiopathy. *Neurology*, *74*(17), 1346–1350. https://doi.org/10.1212/WNL.0b013e3181dad605

Nitkunan, A., Barrick, T. R., Charlton, R. a., Clark, C. a., & Markus, H. S. (2008). Multimodal MRI in cerebral small vessel disease: Its relationship with cognition and sensitivity to change over time. *Stroke*, *39*(7), 1999–2005. https://doi.org/10.1161/STROKEAHA.107.507475

Patel, B., & Markus, H. S. (2011). Magnetic resonance imaging in cerebral small vessel disease and its use as a surrogate disease marker. *International Journal of Stroke*, *6*(1), 47–59. https://doi.org/10.1111/j.1747-4949.2010.00552.x

Reijmer, Y. D., Fotiadis, P., Martinez-Ramirez, S., Salat, D. H., Schultz, A., Shoamanesh, A., … Greenberg, S. M. (2015). Structural network alterations and neurological dysfunction in cerebral amyloid angiopathy. *Brain*, *138*(1), 179–188. https://doi.org/10.1093/brain/awu316

Rosand, J., Hylek, E. M., O'Donnell, H. C., & Greenberg, S. M. (2000). Warfarin-associated hemorrhage and cerebral amyloid angiopathy: a genetic and pathologic study. *Neurology*, *55*(7), 947–951. https://doi.org/10.1212/WNL.55.7.947

Viswanathan, A., Patel, P., Rahman, R., Nandigam, R. N. K., Kinnecom, C., Bracoud, L., … Smith, E. E. (2008). Tissue microstructural changes are independently associated with cognitive impairment in cerebral amyloid angiopathy. *Stroke*, *39*(7), 1988–1992. https://doi.org/10.1161/STROKEAHA.107.509091

Wardlaw, J. M., Smith, E. E., Biessels, G. J., Cordonnier, C., Fazekas, F., Frayne, R., … Dichgans, M. (2013). Neuroimaging standards for research into small vessel disease and its contribution to ageing and neurodegeneration. *The Lancet Neurology*, *12*(8), 822–838.https://doi.org/10.1016/S1474-4422(13)70124-8

Appendix

Publications

Duering, M., Finsterwalder, S., **Baykara, E**., Tuladhar, A. M., Gesierich, B., Konieczny, M. J., Malik, R., Franzmeier, N., Ewers, M., Jouvent, E., Biessels, G. J., Schmidt, R., de Leeuw, F.E., Pasternak, O. & Dichgans, M. (2018). Free water determines diffusion alterations and clinical status in cerebral small vessel disease. *Alzheimer's & dementia: the journal of the Alzheimer's Association*.

Duering, M., Tiedt, S., **Baykara, E**., Lyrer, P., Engelter, S., Gesierich, B., Achmüller, M., Barro, C., Adam, R., Ewers, M., Dichgans, M., Kuhle, J. & Peters, N. (2017). Neurofilament light chain as a serum marker for cerebral small vessel disease (P2. 096).

Baykara, E.*, Wollenweber, F. A.*, Zedde, M., Gesierich, B., Achmüller, M., Jouvent, E., Viswanathan, A., Ropele, S., Chabriat, H., Schmidt, R., Opherk, C., Dichgans, M., Linn, J. & Duering, M. (2017). Cortical superficial siderosis in different types of cerebral small vessel disease. Stroke, 48(5), 1404-1407.

Franzmeier, N., Caballero, M. A., Taylor, A. N. W., Simon-Vermot, L., Buerger, K., Ertl-Wagner, B., Mueller, C., Catak, C., Janowitz, D., **Baykara, E.**, Gesierich, B., Duering, M., Ewers, M. & ADNI. (2017). Resting-state global functional connectivity as a biomarker of cognitive reserve in mild cognitive impairment. Brain imaging and behavior, 11(2), 368-382.

Baykara, E., Gesierich, B., Adam, R., Tuladhar, A. M., Biesbroek, J. M., Koek, H. L., Ropele, S., Jouvent, E., ADNI, Chabriat, H., Ertl-Wagner, B., Ewers, M., Schmidt, R., de Leeuw, F.-E., Biessels, G.J., Dichgans, M. & Duering, M. (2016). A novel imaging marker for small vessel disease based on skeletonization of white matter tracts and diffusion histograms. Annals of neurology, 80(4), 581-592.

Baykara, E., Ruf, C. A., Fioravanti, C., Käthner, I., Simon, N., Kleih, S. C., Kübler, A. & Halder, S. (2016). Effects of training and motivation on auditory P300 brain–computer interface performance. Clinical Neurophysiology, 127(1), 379-387.

*equal contribution

Eidesstattliche Versicherung/Affidavit

Hiermit versichere ich an Eides statt, dass ich die vorliegende Dissertation **Imaging markers of cerebral small vessel disease** selbstständig angefertigt habe, mich außer der angegebenen keiner weiteren Hilfsmittel bedient und alle Erkenntnisse, die aus dem Schrifttum ganz oder annähernd übernommen sind, als solche kenntlich gemacht und nach ihrer Herkunft unter Bezeichnung der Fundstelle einzeln nachgewiesen habe.

I hereby confirm that the dissertation **Imaging markers of cerebral small vessel disease** is the result of my own work and that I have only used sources or materials listed and specified in the dissertation.

München, den 22.11.2018

Munich, date 22.11.2018 Unterschrift signature

Ebru Baykara

Declaration of author contributions

(1) **Baykara, E**., Gesierich, B., Adam, R., Tuladhar, A. M., Biesbroek, J. M., Koek, H. L., Ropele, S., Jouvent, E., ADNI, Chabriat, H., Ertl-Wagner, B., Ewers, M., Schmidt, R., de Leeuw, F.-E., Biessels, G.J., Dichgans, M. & Duering, M. (2016). A novel imaging marker for small vessel disease based on skeletonization of white matter tracts and diffusion histograms. Annals of neurology, 80(4), 581-592.

Author contributions: Study concept and design: E. B., M. Du.; data acquisition: all authors, data analysis: E. B., M. Du, drafting the manuscript and figures: E. B., M. Du.

München, den

Ebru Baykara Marco Duering

(2) **Baykara, E**.*, Wollenweber, F. A.*, Zedde, M., Gesierich, B., Achmüller, M., Jouvent, E., Viswanathan, A., Ropele, S., Chabriat, H., Schmidt, R., Opherk, C., Dichgans, M., Linn, J. & Duering, M. (2017). Cortical superficial siderosis in different types of cerebral small vessel disease. Stroke, 48(5), 1404-1407.

Author contributions: Study concept and design: E. B., F.A.W., M. Du.; data acquisition: all authors, data analysis: E. B., F.A.W., drafting the manuscript and figures: E. B., F.A.W., M. Du.; F.A.W. and E. B. contributed equally.

München, den

Ebru Baykara Frank Arne Wollenweber Marco Duering